Linear Algebra and its Applications ••• (••••) •••–•••

Contents lists available at ScienceDirect

Linear Algebra and its Applications

journal homepage: www.elsevier.com/locate/laa

A maximal distribution result and numerical tests for geometric means of HPD GLT matrix-sequences with degenerate commuting/non-commuting GLT symbols

Asim Ilyas [a], Muhammad Faisal Khan [a,*], Valerio Loi [a], Stefano Serra-Capizzano [a,b]

[a] *Department of Science and High Technology, University of Insubria, Como, 22100, Italy*
[b] *Department of Information Technology, Uppsala University, Uppsala, 75310, Sweden*

ARTICLE INFO

Article history:
Received 3 July 2025
Received in revised form 20 July 2025
Accepted 3 August 2025
Available online xxxx
Submitted by R. Brualdi

MSC:
47A64
47B35
15A18
15B48
39A12
65N

Keywords:
Geometric mean
Matrix theory
Matrix analysis

ABSTRACT

In the current work, we consider the study of the spectral distribution of the geometric mean of two matrix-sequences $\{G(A_n, B_n)\}_n$ formed by Hermitian Positive Definite (HPD) matrices. We assume that the two input matrix-sequences $\{A_n\}_n, \{B_n\}_n$ belong to the same d-level r-block Generalized Locally Toeplitz (GLT) $*$-algebra, with $d, r \geq 1$ and with GLT symbols κ, ξ. Building on recent results in the literature, we examine whether it is necessary to assume that at least one of the input GLT symbols is invertible almost everywhere. Since inversion is mainly required due to the non-commutativity of the matrix product, it was conjectured that the hypothesis on the invertibility of the GLT symbols can be removed. In fact, we prove the conjectured statement in Garoni and Serra-Capizzano (2017) [21, Conjecture 10.1], that is, the sequence of geometric means $\{G(A_n, B_n)\}_n$ is a GLT sequence whose symbol is given by the geometric mean of symbols κ and ξ (i.e., $(\kappa\xi)^{1/2}$), when the symbols κ and ξ commute. This includes the important case where $r = 1$ and $d \geq 1$.

* Corresponding author.
E-mail addresses: ailyas1@uninsubria.it (A. Ilyas), mfkhan@uninsubria.it (M.F. Khan), vloi@uninsubria.it (V. Loi), s.serracapizzano@uninsubria.it, stefano.serra@it.uu.se (S. Serra-Capizzano).

https://doi.org/10.1016/j.laa.2025.08.004

Please cite this article in press as: A. Ilyas et al., A maximal distribution result and numerical tests for geometric means of HPD GLT matrix-sequences with degenerate commuting/non-commuting GLT symbols, Linear Algebra Appl. (2025), https://doi.org/10.1016/j.laa.2025.08.004

Spectral theory
GLT matrix sequences
Momentary symbols
Algebraic structures
Matrix means

Conversely, the statement is generally false or even not well posed, when the symbols are not invertible almost everywhere and do not commute. In fact, numerical experiments are conducted in the case where the two symbols do not commute, showing that the main results of the present work are maximal. Further numerical experiments, visualizations, and conclusions complete the present contribution.

1. Introduction

The concept of the matrix geometric mean has attracted considerable attention from a large number of researchers in recent decades due to its elegant theoretical foundations and growing significance in a wide range of fields, including mathematics, engineering, and applied sciences. More in detail, matrix geometric means appear in diffusion tensor imaging (DTI) [7], radar detection [49,25], image processing [32], elasticity [27], machine learning [23], brain-computer interfaces [50], network analysis [20], and many more applications. Initially the notion of matrix geometric mean was introduced implicitly in the context of a functional calculus for sesquilinear maps by Pusz and Woronowicz [31]. Then it became known as a mean after the work of Kubo and Ando [24]. In this work the matrix geometric mean was rigorously formalized as follows: for two positive definite matrices A and B the geometric mean $G(A, B)$ is defined as

$$G(A,B) = A^{\frac{1}{2}}(A^{-\frac{1}{2}}BA^{-\frac{1}{2}})^{\frac{1}{2}}A^{\frac{1}{2}} = G(B,A).$$

The rigorous definition has been analyzed by Ando, Li, and Mathias (ALM) [2], who also identified the essential axiomatic properties [[12], Section 3], that a proper matrix geometric mean should satisfy: see also [28,26,13,11] and references therein for relevant discussions and studies.

Given a square matrix $A \in \mathbb{C}^{m\times m}$ ($m \geq 1$), we list its eigenvalues, counted with algebraic multiplicity, as $\lambda_1(A), \ldots, \lambda_m(A)$. Its singular values, arranged in non-increasing order, are $\sigma_1(A) \geq \cdots \geq \sigma_m(A) \geq 0$. We write $C_c(\mathbb{R})$ (respectively, $C_c(\mathbb{C})$) for the space of continuous, complex-valued functions on $\mathbb{R}$ (respectively, $\mathbb{C}$) whose support is compact. We use this notation throughout.

Matrix-sequences with explicit or hidden (asymptotic) structure

In recent years, there has been a growing interest in matrix-sequences and on the singular value and eigenvalue distributions in the sense of Weyl, according to the definition below.

Please cite this article in press as: A. Ilyas et al., A maximal distribution result and numerical tests for geometric means of HPD GLT matrix-sequences with degenerate commuting/non-commuting GLT symbols, Linear Algebra Appl. (2025), https://doi.org/10.1016/j.laa.2025.08.004

Definition 1. Let $\{A_n\}_n$ be a matrix-sequence, where A_n is of size d_n, $d_k < d_{k+1}$ for every k, and let $\psi : D \subset \mathbb{R}^t \to \mathbb{C}^{r\times r}$ be a measurable function defined on a set D with $0 < \mu_t(D) < \infty$, $r, t \geq 1$.

- We say that $\{A_n\}_n$ has an **(asymptotic) singular value distribution** described by ψ, written as $\{A_n\}_n \sim_\sigma \psi$, if

$$\lim_{n\to\infty} \frac{1}{d_n} \sum_{i=1}^{d_n} F(\sigma_i(A_n)) = \frac{1}{\mu_t(D)} \int_D \frac{\sum_{i=1}^{r} F(\sigma_i(\psi(\mathbf{x})))}{r} d\mathbf{x}, \quad \forall F \in C_c(\mathbb{R}).$$

- We say that $\{A_n\}_n$ has an **(asymptotic) spectral (eigenvalue) distribution** described by ψ, written as $\{A_n\}_n \sim_\lambda \psi$, if

$$\lim_{n\to\infty} \frac{1}{d_n} \sum_{i=1}^{d_n} F(\lambda_i(A_n)) = \frac{1}{\mu_t(D)} \int_D \frac{\sum_{i=1}^{r} F(\lambda_i(\psi(\mathbf{x})))}{r} d\mathbf{x}, \quad \forall F \in C_c(\mathbb{C}).$$

If ψ describes both singular value and eigenvalue distribution of $\{A_n\}_n$, we write $\{A_n\}_n \sim_{\sigma,\lambda} \psi$.
In this case, the function ψ is referred to as the *eigenvalue (or spectral) symbol* of $\{A_n\}_n$.

The informal meaning behind the spectral distribution definition is discussed in [[1], Section 2.3].

There exist several matrix-sequences with explicit or hidden (asymptotic) structure widely studied in the literature as reported in [9]. Among them we have the d-level r-block Toeplitz matrix-sequences, which have an explicit structure and which enjoy a Szegö-like relation as in Definition 1; see [46] and references therein. They have been studied deeply in the last century, both for their mathematical beauty and for their pervasive use in applications (see e.g. [14,29,46] and references therein). A wide generalization is represented by the notion of generalized locally Toeplitz (GLT) matrix-sequences [40, 41,45], which have inherent hidden structure and which form $*$-algebras. These GLT $*$-algebras include virtually any approximation via local numerical methods of (systems of) partial and fractional differential equations, also with non-smooth variable coefficients and irregular bounded domains/manifolds (see [21,22,4,5] and references therein).

For our work, we consider three types of matrix structures that serve as the fundamental building blocks of the various GLT $*$-algebras [21,22,4,5]: d-level r-block Toeplitz matrix-sequences as given in [[1], Section 2.7], sampling diagonal matrix-sequences [[1], Section 2.8], along with asymptotic structures described by zero-distributed matrix-sequences [[1], Section 2.6].

Specifically, for any positive integers d and r, we consider the set of d-level r-block GLT matrix-sequences. For a matrix-sequence $\{A_n\}_n$ in this set and a measurable function κ, we write $\{A_n\} \sim_{\text{GLT}} \kappa$ to mean that κ is the GLT *symbol* of the sequence. According to

Please cite this article in press as: A. Ilyas et al., A maximal distribution result and numerical tests for geometric means of HPD GLT matrix-sequences with degenerate commuting/non-commuting GLT symbols, Linear Algebra Appl. (2025), https://doi.org/10.1016/j.laa.2025.08.004

the theory, if κ is the GLT symbol of $\{A_n\}_n$ then $\{A_n\}_n \sim_\sigma \kappa$ as in Definition 1. Furthermore, the GLT symbol is also the spectral symbol i.e. $\{A_n\}_n \sim_\lambda \kappa$ if the matrices A_n are Hermitian; see [21,22,4,5] for more details. Given $d, r \geq 1$, the set of d-level r-block GLT matrix-sequences forms a $*$-algebra of matrix-sequences, which is both maximal and isometrically equivalent to the maximal $*$-algebra of $2d$-variate $r \times r$ matrix-valued measurable functions (with respect to the Lebesgue measure) that are naturally defined over $[0,1]^d \times [-\pi,\pi]^d$; see [4,5,21,22] and references therein.

The reduced version of this structure plays a crucial role in approximating integro-differential operators, including their fractional versions, particularly when defined over general (non-Cartesian) domains. This concept was first introduced in [40,41] and later extensively developed in [6], where the GLT symbols are defined again as measurable functions over $\Omega \times [-\pi,\pi]^d$, with Ω being Peano–Jordan measurable and contained within $[0,1]^d$. Additionally, the reduced versions also form maximal $*$-algebras that are isometrically equivalent to their corresponding maximal $*$-algebras of measurable functions.

These GLT $*$-algebras provide a rich framework of hidden (asymptotic) structures, built upon two fundamental classes of explicit algebraic structures (d-level r-block Toeplitz matrix-sequences and sampling diagonal matrix-sequences) and upon the asymptotic structures described by zero-distributed matrix-sequences. Notably, the latter class serves an analogous role to compact operators in relation to bounded linear operators, forming a two-sided ideal of matrix-sequences within any of the GLT $*$-algebras.

We follow the formulation in [[1], Section 2.9]; see also [21,22,4,5] for the original sources.

Main results

An initial spectral study of the geometric mean of structured matrix-sequences was carried out in [[21], Section 10.3], where the spectral properties of HPD GLT matrix-sequences with $r = d = 1$ were analyzed in the context of geometric means and two related conjectures were proposed. Then in [1] the results in [[21], Section 10.3] have been extended to the case of d-level r-block GLT matrix-sequences and the conjectures in [[21], Section 10.3] have been extended. In fact in [1], the authors first established that for two HPD d-level GLT matrix-sequences $\{A_n\}_n \sim_{\text{GLT}} \kappa$ and $\{B_n\}_n \sim_{\text{GLT}} \xi$, their geometric mean also forms a GLT sequence with the symbol $\{G(A_n, B_n)\}_n \sim_{\text{GLT}} (\kappa\xi)^{1/2}$, as rigorously proven in [[1], Theorem 3, Theorem 4], under the assumption that either κ or ξ are nonzero almost everywhere. This result was generalized to d-level r-block GLT sequences in [[1], Theorem 5], extending its applicability to the case where the symbols κ and ξ do not necessarily commute. In that case, we have again $\{G(A_n, B_n)\}_n \sim_{\text{GLT}} G(\kappa, \xi)$, again under the assumption either κ or ξ are invertible almost everywhere. However, in [1] the two conjectures in [[21], Section 10.3] were not solved.

Building on our previous results [1], this work further investigates the necessity of the assumption that at least one of the input GLT symbols is invertible almost everywhere. This assumption was initially introduced to ensure that the inverse of a GLT matrix-sequence remains within the GLT framework. However, since inversion is primar-

Please cite this article in press as: A. Ilyas et al., A maximal distribution result and numerical tests for geometric means of HPD GLT matrix-sequences with degenerate commuting/non-commuting GLT symbols, Linear Algebra Appl. (2025), https://doi.org/10.1016/j.laa.2025.08.004

ily required due to the non-commutativity of matrices, we explore whether this condition can be relaxed in cases where the symbols commute, in the context of d-level r-block GLT matrix-sequences, $d, r \geq 1$. We formally prove that the invertibility assumption on the GLT symbols can be removed when the GLT symbols commute, which includes the case where $r = 1$ and $d \geq 1$, so proving completely [[21], Conjecture 10.1]. In the general setting, we perform extensive numerical experiments. The numerical tests suggest that the requirement of invertibility is essential, showing that our results are maximal when $r > 1$. In fact, for $r > 1$ we report and discuss several cases in which $G(A_n, B_n)$ is well defined for any n, $\{A_n\}_n \sim_{\text{GLT}} \kappa$, $\{B_n\}_n \sim_{\text{GLT}} \xi$, the GLT symbols κ, ξ do not commute and are both zero in two positive measure sets, respectively: when each symbol vanishes in a set of positive measure, we refer to them as degenerate symbols. In the degenerate non-commuting case, the resulting observation is that

$$\{G(A_n, B_n)\}_n \sim_{\text{GLT}} \psi,$$

but ψ does not coincide with $G(\kappa, \xi)$ or even $G(\kappa, \xi)$ is not well defined.

Further numerical experiments are also conducted to investigate finer spectral aspects. More precisely, we study the relationships between the order to zeros of the geometric mean of the symbols minus its minimum and the convergence speed to this minimum of the minimal eigenvalue of the geometric mean of the corresponding GLT matrix-sequences. This asymptotical behavior mimicks what is known in the Toeplitz setting [33,34,18,35,36,43] and in the GLT setting [8,42], thus opening new directions for generalizing the existing GLT theory. Notably, in additional numerical tests, e.g., when the product $\kappa\xi$ is equal to zero, the eigenvalue distribution of the geometric mean obtained numerically seems to possess a richer structure. More specifically, the experiments show that the resulting asymptotic spectra can be described by exploiting the theory of GLT momentary symbols, according to [16,17,3].

Structure of the work

The present study is structured as follows. In Section 2, we introduce notations, terminology, and preliminary results related to the notion of the approximating class of sequences [39], essential for the mathematical formulation and technical solution of the problem. In Section 3, we present the main results where we drop the assumption that at least one GLT symbol is invertible almost everywhere when the symbols commute, which includes the case of $d \geq 1, r = 1$ and solves Conjecture 10.1 in [21]. In Section 4, we present numerical experiments illustrating the asymptotic spectral behavior of the geometric mean for GLT matrix-sequences both in the 1D and 2D cases, considering both scalar and block structures. In particular we give evidence of the extremal spectral behavior, of the emergence of GLT momentary symbols phenomena, and more importantly we give evidence that the results of Section 3 are maximal, since the case of degenerate, non-commuting GLT symbols ($r > 1$) leads to noncanonical distribution results. Finally, in Section 5, we draw conclusions and highlight several problems for future research.

Please cite this article in press as: A. Ilyas et al., A maximal distribution result and numerical tests for geometric means of HPD GLT matrix-sequences with degenerate commuting/non-commuting GLT symbols, Linear Algebra Appl. (2025), https://doi.org/10.1016/j.laa.2025.08.004

2. Spectral tools

In this section, we introduce the essential tools for the spectral analysis of the matrices under consideration, using the multi-level block GLT matrix-sequence framework. The case of scalar values, corresponding to the non-block setting, has been extensively detailed in [21,22], while the block setting, associated with matrix-valued symbols, is thoroughly examined in [4,5]. In our specific context, where the block size is $r = 1$ and the problem domain has a dimensionality of $d = 2$, we operate within the realm of two-level non-block GLT sequences.

2.1. Notation and terminology

Matrices and matrix-sequences. Given a square matrix $A \in \mathbb{C}^{m\times m}$, we denote by A^* its conjugate transpose and by $A^\dagger$ the Moore–Penrose pseudoinverse of A. Recall that $A^\dagger = A^{-1}$ whenever A is invertible.
Regarding matrix norms, $\|\cdot\|$ refers to the spectral norm, and for $1 \le p \le \infty$, the notation $\|\cdot\|_p$ stands for the Schatten p-norm defined as the p-norm of the vector of singular values. Note that the Schatten ∞-norm, which is equal to the largest singular value, coincides with the spectral norm $\|\cdot\|$; the Schatten 1-norm since it is the sum of the singular values is often referred to as the trace-norm; and the Schatten 2-norm coincides with the Frobenius norm. Schatten p-norms, as important special cases of unitarily invariant norms, are treated in detail in a wonderful book by Bhatia [10].
Finally, the expression **matrix-sequence** refers to any sequence of the form $\{A_n\}_n$, where A_n is a square matrix of size d_n, with $d_k < d_{k+1}$ for every k, so that $d_n \to \infty$ as $n \to \infty$. A **r-block matrix-sequence**, or simply a matrix-sequence if r can be deduced from context, is a special $\{A_n\}_n$ in which the size of A_n is $d_n = r\varphi_n$, with $r \ge 1 \in \mathbb{N}$ fixed and $\varphi_n \in \mathbb{N}$ such that $\varphi_k < \varphi_{k+1}$ for every k.

2.2. Multi-index notation

To effectively deal with multilevel structures, it is necessary to use multi-indices, which are vectors of the form $\mathbf{i} = (i_1, \cdots, i_d) \in \mathbb{Z}^d$. The related notation is listed below.

- $\mathbf{0}, \mathbf{1}, \mathbf{2}, \ldots$ are vectors of all zeroes, ones, twos, etc.
- $\mathbf{h} \le \mathbf{k}$ means that $h_r \le k_r$ for all $r = 1, \cdots, d$. In general, relations between multi-indices are evaluated componentwise.
- Operations between multi-indices, such as addition, subtraction, multiplication, and division, are also performed componentwise.
- The multi-index interval $[\mathbf{h}, \mathbf{k}]$ is the set $\{\mathbf{j} \in \mathbb{Z}^d : \mathbf{h} \le \mathbf{j} \le \mathbf{k}\}$. We always assume that the elements in an interval $[\mathbf{h}, \mathbf{k}]$ are ordered in the standard lexicographic manner

Please cite this article in press as: A. Ilyas et al., A maximal distribution result and numerical tests for geometric means of HPD GLT matrix-sequences with degenerate commuting/non-commuting GLT symbols, Linear Algebra Appl. (2025), https://doi.org/10.1016/j.laa.2025.08.004

$$\left[\cdots\left[\left[(j_1,\cdots,j_d)\right]_{j_d=h_d,\cdots,k_d}\right]_{j_{d-1}=h_{d-1},\cdots,k_{d-1}}\cdots\right]_{j_1=h_1,\cdots,k_1}.$$

- $\mathbf{j}=\mathbf{h},\cdots,\mathbf{k}$ means that $\mathbf{j}$ varies from $\mathbf{h}$ to $\mathbf{k}$, always following the lexicographic ordering.
- $\mathbf{m}\to\infty$ means that $\min(\mathbf{m})=\min_{j=1,\cdots,d} m_j\to\infty$.
- The product of all the components of $\mathbf{m}$ is denoted as $\nu(\mathbf{m}):=\prod_{j=1}^{d} m_j$.

A *d*-**level matrix-sequence** is a matrix-sequence $\{A_{\mathbf{n}}\}_n$ such that n varies in some infinite subset of $\mathbb{N}$, $\mathbf{n}=\mathbf{n}(n)$ is a multi-index in $\mathbb{N}^d$ depending on n, and $\mathbf{n}\to\infty$ when $n\to\infty$. This is typical of many approximations of differential operators in d dimensions; see e.g. [5] and references therein.

With reference to Definition 1, the same notions of distribution apply when the considered matrix-sequence shows a multilevel structure; see [47,46,5,22] and references therein. In that case, n is uniformly replaced by $\boldsymbol{n}$ in A_n and d_n.

2.3. Approximating classes of sequences

In this subsection, we present the notion of the approximating class of sequences and a related key result [39]: both can be found in [21], while the foundation of the notion can be traced back to the papers [47,45,38].

Definition 2. (Approximating class of sequences) Let $\{A_n\}_n$ be a matrix-sequence and let $\{\{B_{n,j}\}_n\}_j$ be a class of matrix-sequences, with A_n and $B_{n,j}$ of size d_n, $d_k<d_{k+1}$ for every k. We say that $\{\{B_{n,j}\}_n\}_j$ is an approximating class of sequences (a.c.s.) for $\{A_n\}_n$ if the following conditions are met: for every j, there exists n_j such that, for every $n\geq n_j$, we find

$$A_n=B_{n,j}+R_{n,j}+N_{n,j},$$

where

$$\operatorname{rank}R_{n,j}\leq c(j)d_n,\quad\text{and}\quad\|N_{n,j}\|\leq\omega(j),$$

where n_j, $c(j)$, and $\omega(j)$ depend only on j and

$$\lim_{j\to\infty}c(j)=\lim_{j\to\infty}\omega(j)=0.$$

$\{\{B_{n,j}\}_n\}_j\xrightarrow{\text{a.c.s. wrt } j}\{A_n\}_n$ denotes that $\{\{B_{n,j}\}_n\}_j$ is an a.c.s. for $\{A_n\}_n$.

The following theorem represents the expression of a related convergence theory, and it is a powerful tool used, for example, in the construction of the GLT $*$-algebra.

Please cite this article in press as: A. Ilyas et al., A maximal distribution result and numerical tests for geometric means of HPD GLT matrix-sequences with degenerate commuting/non-commuting GLT symbols, Linear Algebra Appl. (2025), https://doi.org/10.1016/j.laa.2025.08.004

Theorem 1. *Let $\{A_n\}_n, \{B_{n,j}\}_n$, with $j, n \in \mathbb{N}$, be matrix-sequences and let $\psi, \psi_j : D \subset \mathbb{R}^d \to \mathbb{C}$ be measurable functions defined on a set D with positive and finite Lebesgue measure. Suppose that*

1. *$\{B_{n,j}\}_n \sim_\sigma \psi_j$ for every j;*
2. *$\{\{B_{n,j}\}_n\}_j \xrightarrow{a.c.s.\ wrt\ j} \{A_n\}_n$;*
3. *$\psi_j \to \psi$ in measure.*

Then

$$\{A_n\}_n \sim_\sigma \psi.$$

Moreover, if all the involved matrices are Hermitian, the first assumption is replaced by $\{B_{n,j}\}_n \sim_\lambda \psi_j$ for every j, and the other two are left unchanged, then $\{A_n\}_n \sim_\lambda \psi$.

We end this section by observing that the same definition can be given, and corresponding results (with obvious changes) hold, when the involved matrix-sequences show a multilevel structure. In that case n is replaced by $\boldsymbol{n}$ uniformly in $A_n, B_{n,j}, d_n$.

3. Geometric mean of GLT matrix-sequences

We start by recalling Theorem 4 in [1], which generalizes Theorem 10.2 in [21].

Theorem 2. [[1], Theorem 4] *Let $r = 1$ and $d \geq 1$. Suppose $\{A_{\boldsymbol{n}}\}_{\boldsymbol{n}} \sim_{\text{GLT}} \kappa$ and $\{B_{\boldsymbol{n}}\}_{\boldsymbol{n}} \sim_{\text{GLT}} \xi$, where $A_{\boldsymbol{n}}, B_{\boldsymbol{n}} \in \mathcal{P}_{\nu(\boldsymbol{n})}$ for every multi-index $\boldsymbol{n}$, with $\mathcal{P}_{\nu(\boldsymbol{n})}$ denoting the set of Hermitian positive definite (HPD) matrices of multi-index $\boldsymbol{n}$. Assume that at least one of κ and ξ is nonzero almost everywhere. Then*

$$\{G(A_{\boldsymbol{n}}, B_{\boldsymbol{n}})\}_{\boldsymbol{n}} \sim_{\text{GLT}} (\kappa\xi)^{1/2}, \tag{3.1}$$

and

$$\{G(A_{\boldsymbol{n}}, B_{\boldsymbol{n}})\}_{\boldsymbol{n}} \sim_{\sigma,\lambda} (\kappa\xi)^{1/2}. \tag{3.2}$$

Using the topological a.c.s. notion, we now show that the thesis of the previous theorem holds without assuming that at least one between κ and ξ is invertible almost everywhere, thus proving [[21], Conjecture 10.1]. We make use of Axioms **GLT 1.**, **GLT 2.**, **GLT 3.**, **GLT 4.**, **GLT 5.**, **GLT 6.** as reported in [[1], Section 2.9].

Theorem 3. *Let $r = 1$ and $d \geq 1$. Assume $\{A_{\boldsymbol{n}}\}_{\boldsymbol{n}} \sim_{\text{GLT}} \kappa$ and $\{B_{\boldsymbol{n}}\}_{\boldsymbol{n}} \sim_{\text{GLT}} \xi$, where $A_{\boldsymbol{n}}, B_{\boldsymbol{n}} \in \mathcal{P}_{\nu(\boldsymbol{n})}$ for every multi-index $\boldsymbol{n}$. Then*

$$\{G(A_{\boldsymbol{n}}, B_{\boldsymbol{n}})\}_{\boldsymbol{n}} \sim_{\text{GLT}} (\kappa\xi)^{1/2},$$

Please cite this article in press as: A. Ilyas et al., A maximal distribution result and numerical tests for geometric means of HPD GLT matrix-sequences with degenerate commuting/non-commuting GLT symbols, Linear Algebra Appl. (2025), https://doi.org/10.1016/j.laa.2025.08.004

$$\{G(A_{\boldsymbol{n}}, B_{\boldsymbol{n}})\}_{\boldsymbol{n}} \sim_{\sigma,\lambda} (\kappa\xi)^{1/2}.$$

Proof. We have

$$\{A_{\boldsymbol{n}}\}_{\boldsymbol{n}} \sim_{\text{GLT}} \kappa, \tag{3.3}$$

$$\{B_{\boldsymbol{n}}\}_{\boldsymbol{n}} \sim_{\text{GLT}} \xi, \tag{3.4}$$

where $\kappa, \xi : [0,1]^d \times [-\pi,\pi]^d \to \mathbb{C}$ and $A_{\boldsymbol{n}}, B_{\boldsymbol{n}}$ are Hermitian positive definite matrices $\forall \boldsymbol{n}$. Therefore $\kappa, \xi : [0,1]^d \times [-\pi,\pi]^d \to \mathbb{R}_0^+$ almost everywhere: furthermore, we assume that $\mu_{2d}(\kappa \equiv 0) > 0$ and $\mu_{2d}(\xi \equiv 0) > 0$, so that the hypotheses of [[21], Theorem 10.2] for $d = 1$ and of Theorem 2 for $d > 1$ are violated. Let $\varepsilon > 0$, let $\kappa_\varepsilon = \kappa + \varepsilon$ and let $A_{\boldsymbol{n},\varepsilon} = A_{\boldsymbol{n}} + \varepsilon I_{\nu(\boldsymbol{n})}$, where $I_{\nu(\boldsymbol{n})}$ denotes the identity matrix of size $\nu(\boldsymbol{n})$. By the first part of Axiom **GLT 2.** (the identity is a special Toeplitz matrix with GLT symbol 1), we have $\{\varepsilon I_{\nu(\boldsymbol{n})} = T_{\boldsymbol{n}}(\varepsilon)\}_{\boldsymbol{n}} \sim_{\text{GLT}} \varepsilon$, where $T_{\boldsymbol{n}}(\varepsilon)$ denotes the Toeplitz matrix generated by the constant function ε. Now, by exploiting linearity, i.e., the second item of Axiom **GLT 3.**, it follows that

$$\{A_{\boldsymbol{n},\varepsilon}\}_{\boldsymbol{n}} \sim_{\text{GLT}} \kappa_\varepsilon, \quad \kappa_\varepsilon \geq \varepsilon \ \text{ almost everywhere,}$$

since $\kappa, \xi \geq 0$ almost everywhere due to (3.3) and (3.4). Hence, we are again in the framework of Theorem 2. Therefore, by Theorem 2 we conclude that the sequence of geometric means satisfies the GLT relation

$$\{G(A_{\boldsymbol{n},\varepsilon}, B_{\boldsymbol{n}})\}_{\boldsymbol{n}} \sim_{\text{GLT}} (\kappa_\varepsilon \xi)^{\frac{1}{2}}.$$

Furthermore, we apply the full $*$-algebra framework of the GLT matrix-sequences as in [[1], Section 2.9]. More precisely, by the third item of Axiom **GLT 3.** followed by Axiom **GLT 6.** with the function $f(z) = z^{\frac{1}{4}}$, we obtain

$$\{(A_{\boldsymbol{n},\varepsilon} B_{\boldsymbol{n}}^2 A_{\boldsymbol{n},\varepsilon})^{\frac{1}{4}}\}_{\boldsymbol{n}} \sim_{\text{GLT}} (\kappa_\varepsilon^2 \xi^2)^{\frac{1}{4}} = (\kappa_\varepsilon \xi)^{\frac{1}{2}},$$

which the very same GLT symbol of $\{G(A_{\boldsymbol{n},\varepsilon}, B_{\boldsymbol{n}})\}_{\boldsymbol{n}}$. As a result, again by the second item of Axiom **GLT 3.**, the difference between these sequences satisfies the following asymptotic GLT relation

$$\{G(A_{\boldsymbol{n},\varepsilon}, B_{\boldsymbol{n}}) - (A_{\boldsymbol{n},\varepsilon} B_{\boldsymbol{n}}^2 A_{\boldsymbol{n},\varepsilon})^{\frac{1}{4}}\}_{\boldsymbol{n}} \sim_{\text{GLT}} 0. \tag{3.5}$$

The previous relation is the key step since we have found a new GLT matrix-sequence having the same GLT symbol as the geometric mean matrix-sequence $\{G(A_{\boldsymbol{n},\varepsilon}, B_{\boldsymbol{n}})\}_{\boldsymbol{n}}$, but where no inversion is required. Now given the structure of the performed operations, by virtue of Definition 2, the class $\{\{(A_{\boldsymbol{n},\varepsilon} B_{\boldsymbol{n}}^2 A_{\boldsymbol{n},\varepsilon})^{\frac{1}{4}}\}_{\boldsymbol{n}}, \varepsilon > 0\}$ is obviously an a.c.s. for $\{(A_{\boldsymbol{n}} B_{\boldsymbol{n}}^2 A_{\boldsymbol{n}})^{\frac{1}{4}}\}_{\boldsymbol{n}}$. As a consequence, by invoking (3.5), also the class

Please cite this article in press as: A. Ilyas et al., A maximal distribution result and numerical tests for geometric means of HPD GLT matrix-sequences with degenerate commuting/non-commuting GLT symbols, Linear Algebra Appl. (2025), https://doi.org/10.1016/j.laa.2025.08.004

$$\{\{G(A_{\boldsymbol{n},\varepsilon}, B_{\boldsymbol{n}})\}_{\boldsymbol{n}}, \varepsilon > 0\}$$

is an a.c.s. for $\{(A_{\boldsymbol{n}}B_{\boldsymbol{n}}^2A_{\boldsymbol{n}})^{\frac{1}{4}}\}_{\boldsymbol{n}}$, with all the involved sequences being GLT matrix-sequences, with symbols $(\kappa_\varepsilon\xi)^{\frac{1}{2}}, (\kappa\xi)^{\frac{1}{2}}$, $\varepsilon > 0$. Therefore, since $\exists \lim_{\varepsilon\to 0}(\kappa_\varepsilon\xi)^{\frac{1}{2}} = (\kappa\xi)^{\frac{1}{2}}$, by using the powerful Theorem 1, we deduce that $\exists \lim_{\varepsilon\to 0}$ (a.c.s.) $\{\{G(A_{\boldsymbol{n},\varepsilon}, B_{\boldsymbol{n}})\}_{\boldsymbol{n}}, \varepsilon\}$ $= \{(A_{\boldsymbol{n}}B_{\boldsymbol{n}}^2A_{\boldsymbol{n}})^{\frac{1}{4}}\}_{\boldsymbol{n}} \sim_{\text{GLT}} (\kappa\xi)^{\frac{1}{2}}$ and this limit coincides with $\{G(A_{\boldsymbol{n}}, B_{\boldsymbol{n}})\}_{\boldsymbol{n}}$ in the a.c.s. topology, that is, $\{G(A_{\boldsymbol{n}}, B_{\boldsymbol{n}}) - (A_{\boldsymbol{n}}B_{\boldsymbol{n}}^2A_{\boldsymbol{n}})^{\frac{1}{4}}\}_{\boldsymbol{n}} \sim_{\text{GLT}} 0$. Finally $\{(A_{\boldsymbol{n}}B_{\boldsymbol{n}}^2A_{\boldsymbol{n}})^{\frac{1}{4}}\}_{\boldsymbol{n}} \sim_{\text{GLT}}$ $(\kappa\xi)^{\frac{1}{2}}$. Hence

$$\{G(A_{\boldsymbol{n}}, B_{\boldsymbol{n}})\}_{\boldsymbol{n}} \sim_{\text{GLT}} (\kappa\xi)^{1/2},$$

so that, by Axiom **GLT 1.**, we infer

$$\{G(A_{\boldsymbol{n}}, B_{\boldsymbol{n}})\}_{\boldsymbol{n}} \sim_{\sigma,\lambda} (\kappa\xi)^{1/2}. \quad \square$$

Remark 1 *(Intuition on the generalization).* One of the basic but key ingredients of the previous proof is that scalar-valued functions commute. Hence, it is reasonable to expect that the same proof also works in the case of d-level r-block GLT matrix-sequences, when assuming that the symbols commute. We collect the result in Theorem 5 whose proof follows verbatim that of Theorem 3, except for minimal changes. On the other hand, when both κ and ξ are not invertible almost everywhere (degenerate) and do not commute, the expression $G(\kappa, \xi)$ is not well defined. In fact, we could replace the inversion with the standard pseudoinversion, which is denoted as X^+ if X is any complex matrix. However, we stress that the expression $\kappa^{\frac{1}{2}}([\kappa^{\frac{1}{2}}]^+\xi[\kappa^{\frac{1}{2}}]^+)^{\frac{1}{2}}\kappa^{\frac{1}{2}}$ is not the same as $\xi^{\frac{1}{2}}([\xi^{\frac{1}{2}}]^+\kappa[\xi^{\frac{1}{2}}]^+)^{\frac{1}{2}}\xi^{\frac{1}{2}}$ in general and this is a serious indication that the commutation between the GLT symbols is essential, when the symbols are both degenerate.

We now recall the result proven in [1], concerning the general GLT setting with $d, r \geq 1$ and when at least one of the involved GLT symbols is invertible almost everywhere.

Theorem 4. [[1], Theorem 5] *Let $r, d \geq 1$. Suppose $\{A_{\boldsymbol{n}}\}_{\boldsymbol{n}} \sim_{\text{GLT}} \kappa$ and $\{B_{\boldsymbol{n}}\}_{\boldsymbol{n}} \sim_{\text{GLT}} \xi$, where $A_{\boldsymbol{n}}, B_{\boldsymbol{n}} \in \mathcal{P}_{\nu(\boldsymbol{n})}$ for every multi-index $\boldsymbol{n}$. Assume that at least one of the minimal eigenvalues of κ and the minimal eigenvalue of ξ is nonzero almost everywhere. Then*

$$\{G(A_{\boldsymbol{n}}, B_{\boldsymbol{n}})\}_{\boldsymbol{n}} \sim_{\text{GLT}} G(\kappa, \xi), \tag{3.6}$$

and

$$\{G(A_{\boldsymbol{n}}, B_{\boldsymbol{n}})\}_{\boldsymbol{n}} \sim_{\sigma,\lambda} G(\kappa, \xi). \tag{3.7}$$

Furthermore $G(\kappa, \xi) = (\kappa\xi)^{1/2}$ whenever the GLT symbols κ and ξ commute.

Theorem 5. *Let $r > 1$ and $d \geq 1$. Assume that $\{A_{\boldsymbol{n}}\}_{\boldsymbol{n}} \sim_{\text{GLT}} \kappa$ and $\{B_{\boldsymbol{n}}\}_{\boldsymbol{n}} \sim_{\text{GLT}} \xi$, where $A_{\boldsymbol{n}}, B_{\boldsymbol{n}} \in \mathcal{P}_{\nu(\boldsymbol{n})}$ for every multi-index $\boldsymbol{n}$, with $\mathcal{P}_{\nu(\boldsymbol{n})}$ denoting the set of Hermitian*

Please cite this article in press as: A. Ilyas et al., A maximal distribution result and numerical tests for geometric means of HPD GLT matrix-sequences with degenerate commuting/non-commuting GLT symbols, Linear Algebra Appl. (2025), https://doi.org/10.1016/j.laa.2025.08.004

positive definite (HPD) matrices of size $r\boldsymbol{n}$. Under the assumption that κ and ξ commute we infer

$$\{G(A_{\boldsymbol{n}}, B_{\boldsymbol{n}})\}_{\boldsymbol{n}} \sim_{\text{GLT}} (\kappa\xi)^{1/2},$$
$$\{G(A_{\boldsymbol{n}}, B_{\boldsymbol{n}})\}_{\boldsymbol{n}} \sim_{\sigma,\lambda} (\kappa\xi)^{1/2}.$$

Proof. Since $\{A_{\boldsymbol{n}}\}_{\boldsymbol{n}} \sim_{\text{GLT}} \kappa$, $\{B_{\boldsymbol{n}}\}_{\boldsymbol{n}} \sim_{\text{GLT}} \xi$, we deduce that $\kappa, \xi : [0,1]^d \times [-\pi,\pi]^d \to \mathbb{C}^{r\times r}$ are Hermitian nonnegative definite, while, by the assumptions, $A_{\boldsymbol{n}}, B_{\boldsymbol{n}}$ are Hermitian positive definite matrices $\forall \boldsymbol{n}$. Therefore, the minimal eigenvalue of κ and the minimal eigenvalues of ξ are nonnegative almost everywhere. Here, we assume that $\mu_{2d}(\lambda_{\min}(\kappa) \equiv 0) > 0$ and $\mu_{2d}(\lambda_{\min}(\xi) \equiv 0) > 0$, in such a way that the hypotheses of Theorem 4 are violated. Let $\varepsilon > 0$, let $\kappa_\varepsilon = \kappa + \varepsilon I_r$, I_r being the identity of size r, and let $A_{\boldsymbol{n},\varepsilon} = A_{\boldsymbol{n}} + \varepsilon I_{\mathcal{P}(\boldsymbol{n})}$. Now $\{\varepsilon I_{\mathcal{P}(\boldsymbol{n})} = T_{\boldsymbol{n}}(\varepsilon I_r)\}_{\boldsymbol{n}} \sim_{\text{GLT}} \varepsilon I_r$ by the first part of Axiom **GLT 2.** (the identity $I_{r\nu(\boldsymbol{n})}$ is a special multilevel block Toeplitz matrix with GLT symbol I_r). Consequently, by exploiting linearity i.e. the second item of Axiom **GLT 3.**, it follows that

$$\{A_{\boldsymbol{n},\varepsilon}\}_{\boldsymbol{n}} \sim_{\text{GLT}} \kappa_\varepsilon, \quad \kappa_\varepsilon \geq \varepsilon I_r \quad \text{almost everywhere.}$$

Since κ, ξ are both nonnegative definite almost everywhere. Hence, by Theorem 4, we have

$$\{G(A_{\boldsymbol{n},\varepsilon}, B_{\boldsymbol{n}})\}_{\boldsymbol{n}} \sim_{\text{GLT}} (\kappa_\varepsilon\xi)^{\frac{1}{2}},$$

since the commutation between κ and ξ implies the commutation between $\kappa_\varepsilon = \kappa + \varepsilon I_r$ and ξ. By exploiting the $*$-algebra features of the GLT matrix-sequences, and specifically the third item of Axiom **GLT 3.** and Axiom **GLT 6.** with the function $f(z) = z^{\frac{1}{4}}$, we deduce $\{(A_{\boldsymbol{n},\varepsilon}B_{\boldsymbol{n}}^2A_{\boldsymbol{n},\varepsilon})^{\frac{1}{4}}\}_{\boldsymbol{n}} \sim_{\text{GLT}} (\kappa_\varepsilon^2\xi^2)^{\frac{1}{4}} = (\kappa_\varepsilon\xi)^{\frac{1}{2}}$, which is the very same GLT symbol of $\{G(A_{\boldsymbol{n},\varepsilon}, B_{\boldsymbol{n}})\}_{\boldsymbol{n}}$. As a result, again by the second item of Axiom **GLT 3.**, the difference between these sequences satisfies the following asymptotic relation

$$\{G(A_{\boldsymbol{n},\varepsilon}, B_{\boldsymbol{n}}) - (A_{\boldsymbol{n},\varepsilon}B_{\boldsymbol{n}}^2A_{\boldsymbol{n},\varepsilon})^{\frac{1}{4}}\}_{\boldsymbol{n}} \sim_{\text{GLT}} 0. \tag{3.8}$$

In other words, we have written a new GLT matrix-sequence having the same symbol as the geometric mean matrix-sequence $\{G(A_{\boldsymbol{n},\varepsilon}, B_{\boldsymbol{n}})\}_{\boldsymbol{n}}$, but where no inversion is required. By virtue of Definition 2, the class $\{\{(A_{\boldsymbol{n},\varepsilon}B_{\boldsymbol{n}}^2A_{\boldsymbol{n},\varepsilon})^{\frac{1}{4}}\}_{\boldsymbol{n}}, \varepsilon > 0\}$ is an a.c.s. for $\{(A_{\boldsymbol{n}}B_{\boldsymbol{n}}^2A_{\boldsymbol{n}})^{\frac{1}{4}}\}_{\boldsymbol{n}}$. Therefore, by (3.8), also the class $\{\{G(A_{\boldsymbol{n},\varepsilon}, B_{\boldsymbol{n}})\}_{\boldsymbol{n}}, \varepsilon > 0\}$ is an a.c.s. for $\{(A_{\boldsymbol{n}}B_{\boldsymbol{n}}^2A_{\boldsymbol{n}})^{\frac{1}{4}}\}_{\boldsymbol{n}}$, with all the involved sequences being GLT matrix-sequences, with symbols $(\kappa_\varepsilon\xi)^{\frac{1}{2}}, (\kappa\xi)^{\frac{1}{2}}$, $\varepsilon > 0$. Since $\exists \lim_{\varepsilon\to 0}(\kappa_\varepsilon\xi)^{\frac{1}{2}} = (\kappa\xi)^{\frac{1}{2}}$, Theorem 1 implies $\exists \lim_{\varepsilon\to 0}$ (a.c.s.) $\{\{G(A_{\boldsymbol{n},\varepsilon}, B_{\boldsymbol{n}})\}_{\boldsymbol{n}}, \varepsilon\} = \{(A_{\boldsymbol{n}}B_{\boldsymbol{n}}^2A_{\boldsymbol{n}})^{\frac{1}{4}}\}_{\boldsymbol{n}} \sim_{\text{GLT}} (\kappa\xi)^{\frac{1}{2}}$. It is now clear that this limit coincides with $\{G(A_{\boldsymbol{n}}, B_{\boldsymbol{n}})\}_{\boldsymbol{n}}$ in the a.c.s. topology, that is, $\{G(A_{\boldsymbol{n}}, B_{\boldsymbol{n}}) - (A_{\boldsymbol{n}}B_{\boldsymbol{n}}^2A_{\boldsymbol{n}})^{\frac{1}{4}}\}_{\boldsymbol{n}} \sim_{\text{GLT}} 0$. In this manner $\{(A_{\boldsymbol{n}}B_{\boldsymbol{n}}^2A_{\boldsymbol{n}})^{\frac{1}{4}}\}_{\boldsymbol{n}} \sim_{\text{GLT}} (\kappa\xi)^{\frac{1}{2}}$.

Please cite this article in press as: A. Ilyas et al., A maximal distribution result and numerical tests for geometric means of HPD GLT matrix-sequences with degenerate commuting/non-commuting GLT symbols, Linear Algebra Appl. (2025), https://doi.org/10.1016/j.laa.2025.08.004

Consequently $\{G(A_{\boldsymbol{n}}, B_{\boldsymbol{n}})\}_{\boldsymbol{n}} \sim_{\text{GLT}} (\kappa\xi)^{1/2}$, so that, by Axiom **GLT 1.**, we finally obtain $\{G(A_{\boldsymbol{n}}, B_{\boldsymbol{n}})\}_{\boldsymbol{n}} \sim_{\sigma,\lambda} (\kappa\xi)^{1/2}$. □

4. Numerical experiments

As is well known, many localization, extremal, and distribution results hold when d-level, r-block Toeplitz matrix-sequences are considered, and these results are somehow summarized in specific analytic features of the generating function of the corresponding matrix-sequence. In turn, the generating function is also the d-variate, $r \times r$ matrix-valued GLT symbol of the d-level, r-block Toeplitz matrix-sequence.

Although the distribution results are also valid for general d-level, r-block GLT matrix-sequences, this is no longer true in general for the extremal behavior and for the localization results, unless we add supplementary assumptions, like the request that the matrix-sequence is obtained via a matrix-valued linear positive operator (LPO) [44,37]. We observe that the geometric mean can be seen as a monotone operator with respect to its two variables, and the monotonicity is implied when we consider an LPO, even if the converse is not true. Hence, it is also interesting to verify which properties are maintained by a geometric mean of two d-level, r-block GLT matrix-sequences in terms of its GLT symbol when it exists.

According to the previous discussion, the remainder of the section considers numerical experiments in the following directions:

- the validation of the distribution results in the commuting setting as in Theorem 3 and Theorem 5;
- connections of the previous results with the notion of Toeplitz and GLT momentary symbols and the extremal behavior compared to the GLT symbol;
- evidence that Theorem 3 and Theorem 5 are maximal, by taking GLT matrix-sequences with non-commuting symbols which are both not invertible almost everywhere.

All numerical experiments are performed using MATLAB R2022b on a laptop equipped with an 11th Gen Intel(R) Core(TM) i5-1155G7 CPU running at 2.50 GHz, with 16 GB of RAM. The operating system was Windows 11 Pro (version 23H2, build 22631.5189).

4.1. Validation of the distribution results

4.1.1. Example 1

Let $d = 1$ and consider the following two matrix-sequences $\{A_n\}_n$, $\{B_n\}_n$, with $A_n = D_n(a) + \frac{1}{n^4} I_n$ and $B_n = T_n(3 + 2\cos(\theta))$, where $T_n(\cdot)$ denotes the Toeplitz operator for $d = 1$, as introduced in [[1], Section 2.7], and, accordingly to [[1], Section 2.8], $D_n(a)$ represents the diagonal matrix generated by the continuous function

Please cite this article in press as: A. Ilyas et al., A maximal distribution result and numerical tests for geometric means of HPD GLT matrix-sequences with degenerate commuting/non-commuting GLT symbols, Linear Algebra Appl. (2025), https://doi.org/10.1016/j.laa.2025.08.004

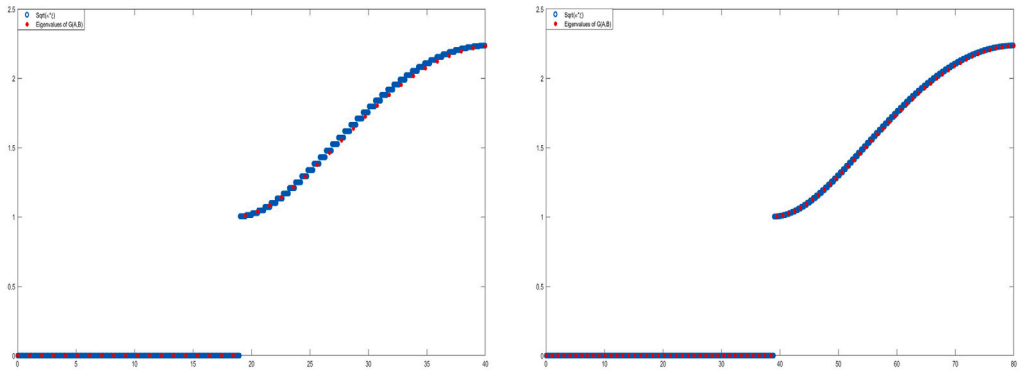

(a) n=40 (b) n=80

Fig. 1. Comparison between the symbol $(\kappa\xi)^{\frac{1}{2}}$ and $\mathrm{eig}(G(A_n, B_n))$.

$$a(x) = \begin{cases} 0, & x \in [0, \frac{1}{2}), \\ 1, & x \in [\frac{1}{2}, 1]. \end{cases}$$

Because of Theorem 3, the geometric mean of these two matrix-sequences, that is $\{G(A_n, B_n)\}_n$, satisfies the GLT relation

$$\{G(A_n, B_n)\}_n \sim_{\mathrm{GLT}} \sqrt{a(x)(3 + 2\cos(\theta))},$$

where the corresponding GLT symbols are explicitly given by $\kappa = a(x)$ and $\xi = 3 + 2\cos(\theta)$.

Eigenvalue distribution

We numerically analyze the spectral behavior of the geometric mean $G(A_n, B_n)$ from **Example 1**. The eigenvalues of this geometric mean are computed for various increasing dimensions n and compared with the uniformly sampled points from the GLT symbol $\sqrt{a(x)(3 + 2\cos(\theta))}$. In Fig. 1, numerical results strongly indicate that the GLT symbol accurately characterizes the eigenvalue distribution of the geometric mean. As n grows, the eigenvalue distribution closely matches the GLT symbol, giving evidence of the theoretical findings in Theorem 3.

4.2. Distribution results and momentary symbols

4.2.1. Example 2

Let $d = 1$ and define the matrix-sequences $\{A_n\}_n$, $\{B_n\}_n$, with $A_n = D_n(a) + \frac{1}{n^4} I_n$, $C_n = T_n(3 + 2\cos(\theta))$ and $B_n = \left(D_n(1-a) + \frac{1}{n^4} I_n\right) C_n \left(D_n(1-a) + \frac{1}{n^4} I_n\right)$, where $D_n(a)$ is the diagonal matrix generated by the piecewise continuous function $a(x)$ given in **Example 1**. Then, the geometric mean sequence explicitly satisfies the GLT relation:

Please cite this article in press as: A. Ilyas et al., A maximal distribution result and numerical tests for geometric means of HPD GLT matrix-sequences with degenerate commuting/non-commuting GLT symbols, Linear Algebra Appl. (2025), https://doi.org/10.1016/j.laa.2025.08.004

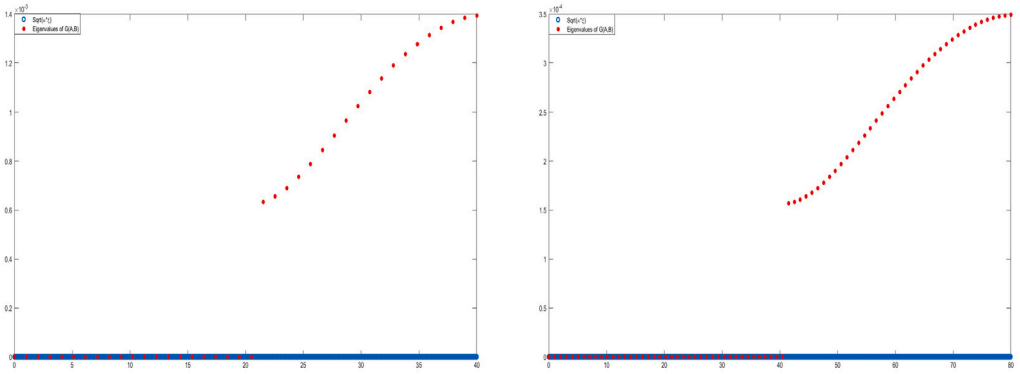

(a) n=40 (b) n=80

Fig. 2. Comparison between the symbol $(\kappa\xi)^{\frac{1}{2}}$ and eig$(G(A_n, B_n))$.

$$\{G(A_n, B_n)\}_n \sim_{\text{GLT}} \sqrt{a(x)(1-a(x))(3+2\cos(\theta))} = a(x)(1-a(x))\sqrt{3+2\cos(\theta)} = 0,$$

where

$$\kappa = a(x) \quad \xi = (1-a(x))(3+2\cos(\theta)).$$

The zero-valued symbol arises naturally due to the definition of the piecewise function $a(x)$:

- For $x \in [0, \frac{1}{2})$, we have $a(x) = 0$. Thus, the term $a(x)(1-a(x))$ becomes zero.
- For $x \in [\frac{1}{2}, 1]$, we have $a(x) = 1$. In this interval, the factor $1-a(x)$ becomes zero, making $a(x)(1-a(x)) = 0$.

Eigenvalue distribution

The eigenvalue distribution of $\{G(A_n, B_n)\}_n$ is numerically analyzed for increasing matrix dimensions n. Since the GLT symbol for this example is zero, by Theorem 3 we expect the eigenvalues to concentrate along the zero line. Interestingly, numerical results reveal an additional spectral structure beyond Theorem 3. For smaller values of n, eigenvalues align closely with zero, as predicted by the GLT symbol. However, some eigenvalues appear above this level, forming a secondary symbol. This phenomenon is attributed to momentary symbols, as discussed in the introduction (see [16,17,3]). As n increases, these elevated eigenvalues shift upwards—reaching approximately 10^{-3} for $n = 40$ (shown in the Fig. 2) and 10^{-4} for $n = 80$.

4.3. Minimal eigenvalues and conditioning

In this section, we analyze the extremal spectral behavior and conditioning of the geometric mean sequence $\{G(A_n, B_n)\}_n$, focusing on its dependence on the analytical properties of the corresponding GLT symbol. This approach follows prior studies

Please cite this article in press as: A. Ilyas et al., A maximal distribution result and numerical tests for geometric means of HPD GLT matrix-sequences with degenerate commuting/non-commuting GLT symbols, Linear Algebra Appl. (2025), https://doi.org/10.1016/j.laa.2025.08.004

Table 1
Numerical behavior of the minimal eigenvalue.

n	τ_j	α_j
40	6.3265×10^{-4}	2.0132
80	1.5673×10^{-4}	2.0064
160	3.9093×10^{-5}	2.0074
320	9.7675×10^{-6}	

on extremal eigenvalues in structured matrix settings, particularly in Toeplitz matrices [18,33,34,43] and block Toeplitz matrices [35,36], as well as variable coefficient differential operators, including multilevel cases with $d > 1$ [48,30,42]. In the case of variable coefficient differential operators, it is worth noticing that extremal spectral results do not stem from the GLT theory but from a combination of GLT tools and properties which are typical of linear positive operators [44,37].

Here, we restrict our attention to the unilevel scalar setting with $d = r = 1$, considering **Example 1** and **Example 2**.

4.3.1. Example 1: minimal eigenvalue

- $X_n = G(A_n, B_n)$
- Take $n_j = 40.2^j, \qquad j = 0, 1, 2, 3,$
- Compute $\tau_j = \lambda_{\min}(X_{n_j}), \qquad j = 0, 1, 2, 3,$
- Compute $\alpha_j = \log_2(\frac{\tau_j}{\tau_{j+1}}), \qquad j = 0, 1, 2.$

As can be seen, the quantity α_j stabilizes around 2 as n increases. This is in perfect agreement with the fact that the minimal eigenvalue of A_n converges to zero as n^{-4}, while the minimal eigenvalue of B_n converges monotonically from above to $\min \xi = 1$. The key point is that the minimal eigenvalue of the geometric mean behaves asymptotically as the geometric mean of the minimal eigenvalues of A_n and B_n, respectively. Similar remarks can be made in the subsequent case regarding **Example 2**.

The observed numerical evidences are not implied by the theoretical derivations, and this is an interesting fact that deserves to be investigated theoretically in the future. In particular, we would like to prove formally that α_j converges to 2 for the first example, Table 1, and it converges to 4 in the second example, Table 2, even from the preliminary numerical results the convergence does not look monotonic.

4.3.2. Example 2: minimal eigenvalue

- $X_n = G(A_n, B_n)$
- Take $n_j = 40.2^j, \qquad j = 0, 1, 2, 3,$
- Compute $\tau_j = \lambda_{\min}(X_{n_j}), \qquad j = 0, 1, 2, 3,$
- Compute $\alpha_j = \log_2(\frac{\tau_j}{\tau_{j+1}}), \qquad j = 0, 1, 2.$

Please cite this article in press as: A. Ilyas et al., A maximal distribution result and numerical tests for geometric means of HPD GLT matrix-sequences with degenerate commuting/non-commuting GLT symbols, Linear Algebra Appl. (2025), https://doi.org/10.1016/j.laa.2025.08.004

Table 2
Numerical behavior of the minimal eigenvalue.

n	τ_j	α_j
40	3.9177×10^{-7}	4.0003
80	2.4480×10^{-8}	4.0040
160	1.5259×10^{-9}	4.0009
320	9.5367×10^{-11}	

4.4. Numerical study: non-commuting, rank-deficient symbols

In this section, through numerical tests, we investigate the eigenvalue distribution of the geometric means $\{G(A_n, B_n)\}_n$ with

$$G(A_n, B_n) \;=\; A_n^{1/2}\big(A_n^{-1/2} B_n A_n^{-1/2}\big)^{1/2} A_n^{1/2},$$

where $\{A_n\}_n$ and $\{B_n\}_n$ are HPD GLT matrix-sequences with $r \times r$ matrix-valued symbols κ, ξ. The GLT matrix-sequences are specifically chosen with GLT symbols so that:

1. they are rank-deficient on a subset of positive Lebesgue measure; and
2. they do not commute pointwise on a set of positive measure.

These hypotheses clearly set the problem outside the scope of commuting or almost everywhere invertible cases treated in Theorem 3 and in Theorem 5.
Our tests provide evidence for two phenomena:

(i) The support of the asymptotic eigenvalue distribution of $\{G(A_n, B_n)\}_n$ coincides with the intersection set $\operatorname{ess}\operatorname{Ran}(\kappa) \cap \operatorname{ess}\operatorname{Ran}(\xi)$; see Section 4.4.2.
(ii) The eigenvalues appear to converge in distribution to a candidate symbol which is rank-deficient and, in general, distinct from the classical geometric mean $G(\kappa, \xi)$.

Clearly, the relation $G(A_n, B_n) \sim_{\mathrm{GLT}} G(\kappa, \xi)$ cannot hold under hypotheses (1.)-(2.), and the experiments show the substantial differences in this case compared to the commuting or invertible scenarios. If this case can be studied within the GLT framework, it requires a more technical application of GLT and a.c.s. theory, along with a deeper functional calculus of matrix means.

4.4.1. Setup of the numerical experiments

Below, we provide the setup of the numerical tests.
We construct four pairs of unilevel GLT matrix-sequences $\{A_n\}_n, \{B_n\}_n$, whose symbols simultaneously satisfy the hypothesis stated at the beginning of Section 4.4 (rank deficiency and non-commutation). They are organized by the property of rank loss:

Please cite this article in press as: A. Ilyas et al., A maximal distribution result and numerical tests for geometric means of HPD GLT matrix-sequences with degenerate commuting/non-commuting GLT symbols, Linear Algebra Appl. (2025), https://doi.org/10.1016/j.laa.2025.08.004

- **Case 1** - each symbol is full rank on a set of positive measure;
- **Case 2** - each symbol is rank-deficient almost everywhere.

Case 1, Example 1.
Define

$$f(\theta) \;=\; \begin{cases} 0, & \theta \in [-\pi, 0], \\ \theta, & \theta \in (0, \pi], \end{cases} \qquad g(\theta) = f(-\theta),$$

and set

$$F(\theta) \;=\; f(\theta) \otimes \begin{bmatrix} 2 & 1 \\ 1 & 2 \end{bmatrix}, \qquad G(\theta) \;=\; g(\theta) \otimes \begin{bmatrix} 3 & 1 \\ 1 & 1 \end{bmatrix}.$$

With the $2n \times 2n$ Toeplitz matrices $T_n(F)$ and $T_n(G)$, define

$$A_n = T_n(F) + \frac{1}{n^3} I_{2n}, \qquad B_n = T_n(G) + \frac{1}{n^3} I_{2n}. \tag{4.1}$$

Case 1, Example 2.
Let $\chi_{[-a,a]}$ be the characteristic function of $[-a, a]$, $0 < a < \pi$, and set

$$\begin{aligned} f(\theta) \;&=\; \chi_{[-1/2,\,1/2]}(\theta), \qquad & g(\theta) \;&=\; \chi_{[-1/4,\,1/4]}(\theta), \\ A \;&=\; \begin{bmatrix} 2 & 1 \\ 1 & 2 \end{bmatrix}, \qquad & B \;&=\; \begin{bmatrix} 3 & 1 \\ 1 & 1 \end{bmatrix}, \\ F(\theta) \;&=\; f(\theta) \otimes A, \qquad & G(\theta) \;&=\; g(\theta) \otimes B. \end{aligned}$$

Define

$$A_n = T_n(F) + \frac{1}{n^3} I_{2n}, \qquad B_n = T_n(G) + \frac{1}{n^3} I_{2n}. \tag{4.2}$$

Case 2, Example 1.
With $f(\theta) = 2 - \cos\theta$, $g(\theta) = 3 + \cos\theta$ and rank one blocks

$$A \;=\; \begin{bmatrix} 1 & 1 \\ 1 & 1 \end{bmatrix}, \qquad B \;=\; \begin{bmatrix} 1 & 2 \\ 2 & 4 \end{bmatrix},$$

let $F(\theta) \;=\; f(\theta) \otimes A$ and $G(\theta) \;=\; g(\theta) \otimes B$. Set

$$A_n = T_n(F) + \frac{1}{n^2} I_{2n}, \qquad B_n = T_n(G) + \frac{1}{n^2} D_n(b), \qquad b(x) = (1 + x) I_2.$$

Here, both symbols are rank 1 almost everywhere.

Please cite this article in press as: A. Ilyas et al., A maximal distribution result and numerical tests for geometric means of HPD GLT matrix-sequences with degenerate commuting/non-commuting GLT symbols, Linear Algebra Appl. (2025), https://doi.org/10.1016/j.laa.2025.08.004

Case 2, Example 2.

Define piecewise-linear scalar functions in $[0,1]$:

$$a(x) \;=\; \begin{cases} 1-2x, & 0 \le x \le \frac{1}{2}, \\ 0, & \frac{1}{2} < x \le 1, \end{cases} \qquad b(x) \;=\; \begin{cases} 0, & 0 \le x \le \frac{1}{3} \text{ or } \frac{2}{3} \le x \le 1, \\ x - \frac{1}{3}, & \frac{1}{3} < x \le \frac{1}{2}, \\ \frac{2}{3} - x, & \frac{1}{2} < x < \frac{2}{3}, \end{cases}$$

and let $D_n(a)$, $D_n(b)$ be the corresponding sampling matrices. With $f(\theta) = 2 + \cos\theta$, $g(\theta) = 3 + \cos\theta$ and

$$A \;=\; \begin{bmatrix} 2 & 0 & 1 \\ 0 & 2 & 1 \\ 1 & 1 & 1 \end{bmatrix}, \qquad B \;=\; \begin{bmatrix} 2 & 1 & 0 \\ 1 & 1 & 1 \\ 0 & 1 & 2 \end{bmatrix},$$

define $F(\theta) \;=\; f(\theta) \otimes A$ and $G(\theta) \;=\; g(\theta) \otimes B$, and set

$$A_n \;=\; \big(D_n^{1/2}(a) \otimes I_3\big)\, T_n(F)\, \big(D_n^{1/2}(a) \otimes I_3\big) + \frac{1}{5n}\, I_{3n}, \tag{4.3}$$

$$B_n \;=\; \big(D_n^{1/2}(b) \otimes I_3\big)\, T_n(G)\, \big(D_n^{1/2}(b) \otimes I_3\big) + \frac{1}{5n}\, I_{3n}. \tag{4.4}$$

In every example we denote by κ and ξ the GLT symbols of $\{A_n\}_n$ and $\{B_n\}_n$, respectively.

4.4.2. A candidate symbol for the geometric mean

Let $\{A_n\}_n$ and $\{B_n\}_n$ be GLT matrix-sequences whose matrix-valued symbols

$$\kappa,\ \xi : [0,1]^d \times [-\pi,\pi]^d \;\longrightarrow\; \mathbb{C}^{\,r\times r},$$

are positive semidefinite.

For any $\varepsilon > 0$ define the strictly positive symbols $\kappa_\varepsilon = \kappa + \varepsilon I_r$, $\xi_\varepsilon = \xi + \varepsilon I_r$. Since the matrix geometric mean is monotone continuous in each argument, the limit below exists point-wise and it is unique ([[2], p. 3]):

Definition 3 *(Candidate symbol).* For almost every (x,θ) set

$$\widetilde{G}(\kappa,\xi)(x,\theta) := \lim_{\varepsilon\to 0} G\big(\kappa_\varepsilon(x,\theta),\, \xi_\varepsilon(x,\theta)\big). \tag{4.5}$$

The matrix-valued symbol $\widetilde{G}(\kappa,\xi)$ is *essentially* positive semidefinite (see [2]) and satisfies the essential support identity

$$\operatorname{ess\,Ran}\, \widetilde{G}(\kappa,\xi) \;=\; \operatorname{ess\,Ran}\big[(x,\theta) \mapsto \operatorname{ran}\kappa(x,\theta) \;\cap\; \operatorname{ran}\xi(x,\theta)\big].$$

Please cite this article in press as: A. Ilyas et al., A maximal distribution result and numerical tests for geometric means of HPD GLT matrix-sequences with degenerate commuting/non-commuting GLT symbols, Linear Algebra Appl. (2025), https://doi.org/10.1016/j.laa.2025.08.004

Here ran M denotes the column space of an individual matrix M, whereas ess Ran(.) is the essential range of a Grassmannian valued measurable map. The essential formulation of the subspace condition can also be formulated as the pre-image of the essential numerical range in the style of [[19], Definition 1].

Taking into account the Definition 3 of the candidate symbol, we propose the following conjecture:

Conjecture 1 *(GLT closure under geometric mean). Let $\{A_n\}_n$ and $\{B_n\}_n$ be Hermitian positive definite GLT matrix-sequences with*

$$\{A_n\}_n \sim_{\text{GLT}} \kappa, \qquad \{B_n\}_n \sim_{\text{GLT}} \xi.$$

Then the geometric mean matrix-sequence is again GLT and

$$\{\, G(A_n, B_n)\,\}_n \ \sim_{\text{GLT}}\ \widetilde{G}(\kappa, \xi),$$

where $\widetilde{G}(\kappa, \xi)$ is the candidate symbol defined in (4.5).

The heuristic justification of the conjecture is the following. For each fixed $\varepsilon > 0$ the shifted sequences $\{A_n + \varepsilon I\}_n$ and $\{B_n + \varepsilon I\}_n$ are GLT sequences symbols κ_ε and ξ_ε and their geometric mean sequences satisfy $\{\, G(A_n + \varepsilon I, B_n + \varepsilon I)\,\}_n \sim_{\text{GLT}} G(\kappa_\varepsilon, \xi_\varepsilon)$. Properties of monotone functions and the matrix geometric mean axioms described in [2], combined with closeness of the GLT $*$-algebra (Axiom **GLT 4**) under a.c.s. convergence, suggest that letting $\varepsilon \to 0$ the limit of $\{\, G(A_n + \varepsilon I, B_n + \varepsilon I)\,\}_n$ is well defined in the a.c.s. topology and this limit is $\{\, G(A_n, B_n)\,\}_n$, up to zero-distributed perturbations, leading to the GLT algebraic part of Conjecture 1, a full proof when κ and ξ do not commute point-wise remains open. Meanwhile, all numerical evidence below supports the conjecture on the spectral distribution part of our hypothesis.

Candidate symbols predicted by Conjecture 1

For the four test pairs introduced in Section 4.4.1, Conjecture 1 predicts the following GLT symbols for $\{G(A_n, B_n)\}_n$. Throughout $\mathbf{1} = (1, 1, 1)^*$, $J = \mathbf{1}\,\mathbf{1}^* \in \mathbb{C}^{3\times 3}$.

Case 1, Example 1

$$\widetilde{G}(\kappa, \xi)(x, \theta) = 0_{2\times 2}.$$

Case 1, Example 2

$$\widetilde{G}(\kappa, \xi)(x, \theta) = \chi_{[-\frac{1}{4}, \frac{1}{4}]}(\theta) \ \otimes C, \qquad C \ = \ \frac{1}{6^{1/4}\sqrt{2+\sqrt{6}}} \begin{bmatrix} 2\sqrt{2}+3\sqrt{3} & \sqrt{2}+\sqrt{3} \\ \sqrt{2}+\sqrt{3} & 2\sqrt{2}+\sqrt{3} \end{bmatrix}.$$

Case 2, Example 1

$$\widetilde{G}(\kappa, \xi)(x, \theta) = 0_{2\times 2}.$$

Please cite this article in press as: A. Ilyas et al., A maximal distribution result and numerical tests for geometric means of HPD GLT matrix-sequences with degenerate commuting/non-commuting GLT symbols, Linear Algebra Appl. (2025), https://doi.org/10.1016/j.laa.2025.08.004

Case 2, Example 2

$$\widetilde{G}(\kappa,\xi)(x,\theta) = \sqrt{\left(2+\cos\theta\right)\left(3+\cos\theta\right)h(x)\,k(x)}\ \otimes J.$$

4.4.3. Numerical verification of the conjecture

Let

$$G_n := G(A_n, B_n) \in \mathbb{C}^{d_n \times d_n}, \qquad d_n = \mathrm{size}(G_n).$$

We test whether the empirical eigenvalue distribution of $\{G_n\}_n$ converges to the distribution induced by the candidate symbol $\widetilde{G}(\kappa,\xi)(x,\theta)$ defined in Section 4.4.2. The comparison follows the standard rearrangement strategy.

1. **Sampling the symbol.** Evaluate $\widetilde{G}(\kappa,\xi)$ on a tensor grid $\{x_j\}_{j=1}^{M_x} \subset [0,1]$, $\{\theta_i\}_{i=1}^{M_\theta} \subset [-\pi,\pi]$ with a total number of $M_x \times M_\theta \simeq 2000$ samples. For each point (x_j,θ_i) compute the r eigenvalues of the function; then merge and sort in non-decreasing order all the computed values. This yields the empirical quantile function of the eigenvalues.
2. **Eigenvalue computation.** Matrices A_n, B_n are generated for $n \in \{40, 80, 160, 320\}$, and eigenvalues are ordered in non-decreasing order, obtaining the quantile spectral distribution function of $\{G_n\}_n$.
   We also record $\lambda_{\min}(G_n)$, $\lambda_{\max}(G_n)$ and the condition number $\mathrm{cond}_2(G_n)$ for later stability analysis.
3. **Quantile plot matching.** For each n we plot the sorted eigenvalues $\left(\lambda_i(G_n)\right)$ against the corresponding rearranged sample values of $\widetilde{G}$. A superposition of the two plots for growing values of n gives an experimental indication of the asymptotic convergence of the empirical spectral distribution of $\{G_n\}_n$ to that of the symbol.
4. **Support analysis.** To estimate the measure of the zero set $\{(x,\theta) : \widetilde{G} = 0\}$ we count the fraction of eigenvalues below the threshold 0.1 compared to the matrix size; the value is an estimate of the complement of the predicted measure of the support as n grows.

All tests for this section are run on an Intel Core Ultra 7 155H CPU (22 threads, 30.9 GiB RAM) under Ubuntu 24.10, Linux 6.11.0-29, with Python 3.12.7, NumPy 1.26.4 and SciPy 1.13.1 linked against OpenBLAS.

Remark 2 *(Measure-theoretic meaning of the rearrangement test).* As anticipated implicitly, the comparison of sorted eigenvalue versus sorted symbol has a precise measure-theoretic foundation based on the quantile approximation theory [15]. For completeness, we report the construction in [15] for the unilevel setting $d = 1$; the multilevel case is analogous.

Please cite this article in press as: A. Ilyas et al., A maximal distribution result and numerical tests for geometric means of HPD GLT matrix-sequences with degenerate commuting/non-commuting GLT symbols, Linear Algebra Appl. (2025), https://doi.org/10.1016/j.laa.2025.08.004

Let r denote the size of the matrix $\widetilde{G}(\kappa,\xi)(x,\theta)$ and put $D = [0,1]\times[-\pi,\pi]$ (so $\mu(D) = 2\pi$). Define the probability space defined by the triple

$$(\Omega, \mathcal{F}, \mathbb{P}), \qquad \Omega = D \times \{1,\dots,m\}, \qquad \mathcal{F} = \mathcal{B}(D) \otimes 2^{\{1,\dots,m\}}.$$

Here, $\mathcal{B}(D)$ denotes the Borel σ-algebra on D, and $2^{\{1,\dots,m\}}$ denotes the power set of $\{1,\dots,m\}$, with product measure $\mathbb{P}(A\times B) = \dfrac{\mu(A)}{2\pi}\,\dfrac{|B|}{r}$.
Introduce the random variable

$$X(x,\theta,i) := \lambda_i\big(\widetilde{G}(\kappa,\xi)(x,\theta)\big), \qquad (x,\theta,i)\in\Omega,$$

where the eigenvalues are ordered nondecreasingly. The quantile function of X is precisely the *non-decreasing rearrangement* $\widetilde{G}^{\dagger}$ of the matrix-valued symbol.
Because spectral distributions are defined only up to measure-preserving rearrangements, we deduce that

$$\{G_n\}_n \sim_\lambda \widetilde{G} \implies \{G_n\}_n \sim_\lambda \widetilde{G}^{\dagger},$$

so verifying convergence to the quantile $\widetilde{G}^{\dagger}$ is equivalent and numerically simpler than verifying convergence to the symbol $\widetilde{G}(\kappa,\xi)$ itself.
Furthermore, whenever $\widetilde{G}^{\dagger}$ is continuous at $t\in(0,1)$, the sorted eigenvalues satisfy $\lambda_{\lceil td_n\rceil}(G_n)\to\widetilde{G}^{\dagger}(t)$ as $n\to\infty$, and the empirical proportion of eigenvalues below a small threshold t_0 (we take $t_0 = 0.1$) converges to $\mathbb{P}[X\le t_0]$, therefore it can be used as an estimate of the measure of the rank-deficient subset $\Big\{(x,\theta) : \lambda_{\min}\Big(\widetilde{G}(\kappa,\xi)(x,\theta)\Big) = 0\Big\}$.

4.4.4. Numerical results

In this section, we compare the sorted eigenvalues of each geometric mean matrix $G(A_n,B_n)$ with the rearranged eigenvalue distribution predicted by the candidate symbol $\widetilde{G}(\kappa,\xi)$. Plots are provided for each block size.

Case 1 Figs. 3–4 display the ordered eigenvalues of $G(A_n,B_n)$ (colored markers) together with the ordered samples of $\widetilde{G}(\kappa,\xi)$ (solid red line).

Example 1. Because the supports of κ and ξ are essentially disjoint, $\widetilde{G}(\kappa,\xi)\equiv 0$. Most of the eigenvalues match the zero line, showing convergence to the zero-distribution. Only a small number of positive outliers remain above the line. For small values of n, the eigenvalue plot appears to be governed by a GLT momentary symbol that, when rearranged, follows a power law that rapidly collapses to the zero function as $n\to\infty$.

Example 2. Here, the supports of κ and ξ intersect in $\theta\in[-0.25,0.25]$. As a result, $\widetilde{G}(\kappa,\xi)$ takes two values: zero outside the overlap and a positive constant matrix inside it. The eigenvalues reflect exactly this behavior: they form a long plateau at zero, followed by two shorter clusters at the positive eigenvalues determined by $\widetilde{G}(\kappa,\xi)$. As we will

Please cite this article in press as: A. Ilyas et al., A maximal distribution result and numerical tests for geometric means of HPD GLT matrix-sequences with degenerate commuting/non-commuting GLT symbols, Linear Algebra Appl. (2025), https://doi.org/10.1016/j.laa.2025.08.004

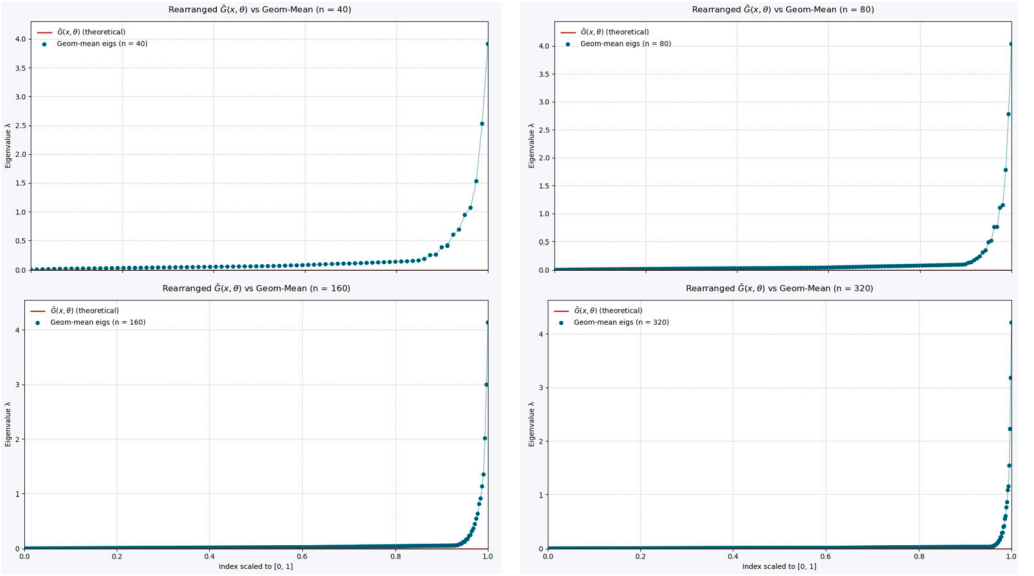

Fig. 3. Case 1 - Example 1. Sorted eigenvalues of $G(A_n, B_n)$ (colored markers; $n = 40, 80, 160, 320$) versus the rearranged distribution of the symbol $\widetilde{G}(\kappa, \xi)$ (solid red line). (For interpretation of the colors in the figure(s), the reader is referred to the web version of this article.)

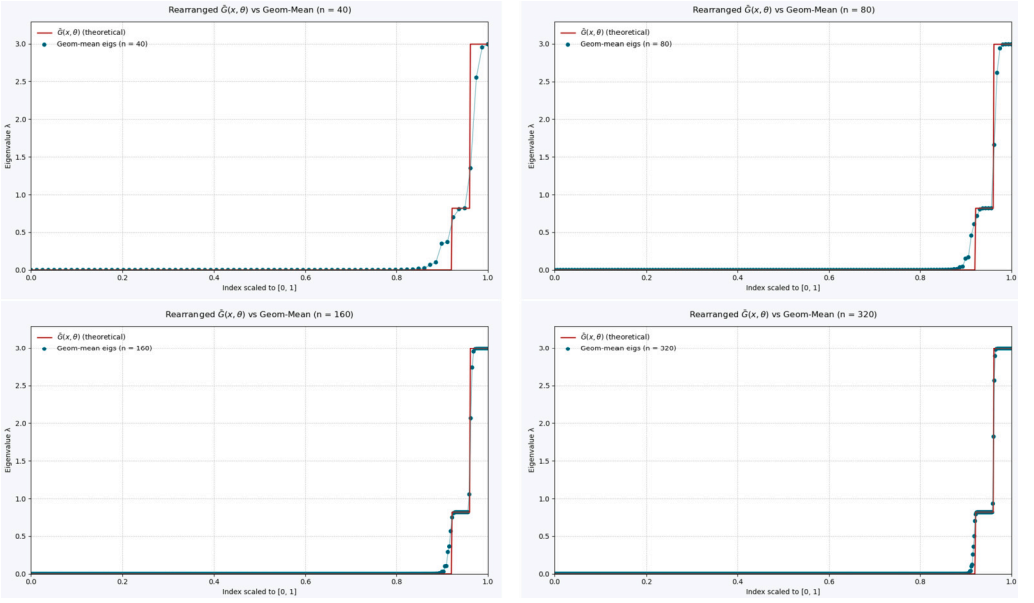

Fig. 4. Case 1 - Example 2. Comparison of the ordered eigenvalues of $G(A_n, B_n)$ (colored markers) with the rearranged values of $\widetilde{G}(\kappa, \xi)$ (solid red line) for $n = 40, 80, 160, 320$.

see, the length of this zero plateau matches the respective Lebesgue measure of the complement of the support of $\widetilde{G}$.

Please cite this article in press as: A. Ilyas et al., A maximal distribution result and numerical tests for geometric means of HPD GLT matrix-sequences with degenerate commuting/non-commuting GLT symbols, Linear Algebra Appl. (2025), https://doi.org/10.1016/j.laa.2025.08.004

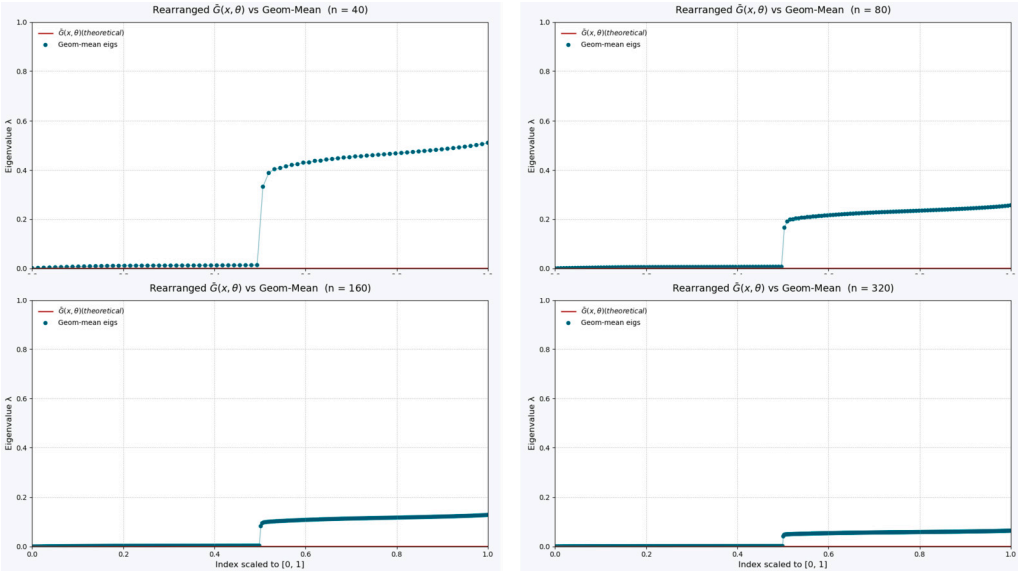

Fig. 5. Case 2, Example 1. Sorted eigenvalues of $G(A_n, B_n)$ (colored markers) versus the rearranged eigenvalue distribution predicted by $G(\kappa, \xi)$ (solid red line), for $n = 40, 80, 160, 320$.

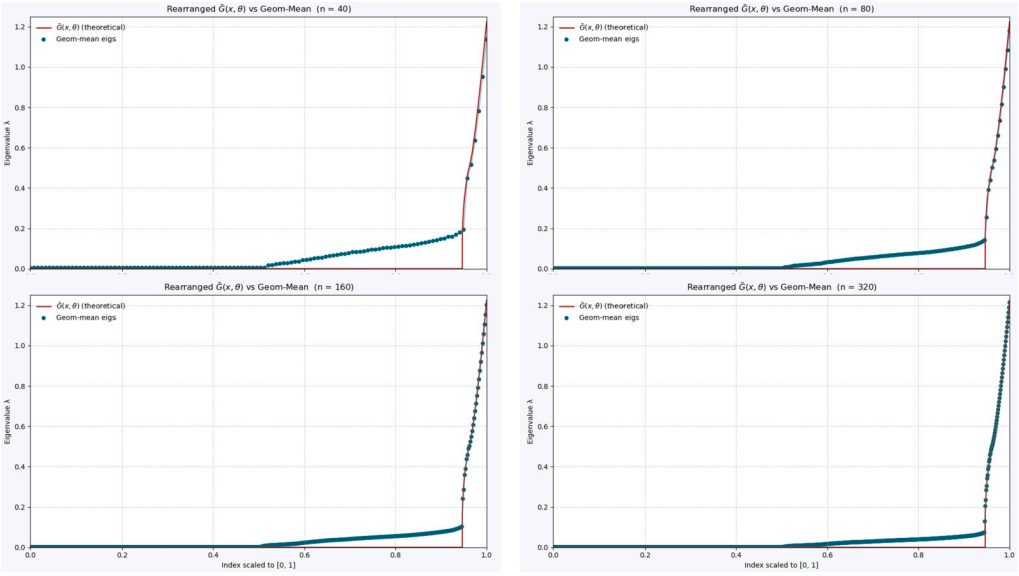

Fig. 6. Case 2, Example 2. Sorted eigenvalues of $G(A_n, B_n)$ (colored markers) versus the rearranged eigenvalue distribution from $G(\kappa, \xi)$ (solid red line), for $n = 40, 80, 160, 320$.

Case 2 Figs. 5–6 repeat the experiment for symbols that are rank-deficient on sets of full measure.

Example 1. Because the supports are disjoint, we have $\widetilde{G}(\kappa, \xi) \equiv 0$. The eigenvalues converge to the zero symbol. Despite the momentary symbol may seem to cause a rougher

Please cite this article in press as: A. Ilyas et al., A maximal distribution result and numerical tests for geometric means of HPD GLT matrix-sequences with degenerate commuting/non-commuting GLT symbols, Linear Algebra Appl. (2025), https://doi.org/10.1016/j.laa.2025.08.004

Table 3
Extremal eigenvalues and condition numbers for **Case 1 - Example 1** (symbol zero almost everywhere).

n	$\widetilde{G}_{\min}$	$\widetilde{G}_{\max}$	Min. eig.	Max. eig.	$\mathrm{cond}_2(G_n)$
40	0.0000	0.0000	8.7142×10^{-3}	3.912 780 29	4.490×10^{2}
80	0.0000	0.0000	3.6849×10^{-3}	4.036 566 85	1.095×10^{3}
160	0.0000	0.0000	1.4929×10^{-3}	4.133 991 29	2.769×10^{3}
320	0.0000	0.0000	5.8335×10^{-4}	4.211 898 05	7.220×10^{3}

Table 4
Extremal eigenvalues and condition numbers for **Case 1 - Example 2** (symbol positive on an overlap set).

n	$\widetilde{G}_{\min}$	$\widetilde{G}_{\max}$	Min. eig.	Max. eig.	$\mathrm{cond}_2(G_n)$
40	0.0000	2.993 930 66	1.5625×10^{-5}	2.992 574 15	1.915×10^{5}
80	0.0000	2.993 930 66	1.9531×10^{-6}	2.993 932 80	1.533×10^{6}
160	0.0000	2.993 930 66	2.4414×10^{-7}	2.993 930 94	1.226×10^{7}
320	0.0000	2.993 930 66	3.0518×10^{-8}	2.993 930 70	9.811×10^{7}

perturbation, we remark that, unlike in Case 1 - Example 1, this perturbation does not result in proper outliers since all perturbed eigenvalues converge to zero. In practice, we observe better convergence.

Example 2. Here, the intersection set has rank one, leading to exactly one positive eigenvalue in $\widetilde{G}(\kappa, \xi)$. The plot shows convergence despite the rank deficiency of the support. Because the norm of the diagonal perturbation introduced in Equation (4.3) decays slowly, a momentary GLT perturbation [3,17] is still observed even in this non-zero case.

Extremal eigenvalues For each block size n we report

$$\lambda_{\min}(G_n), \qquad \lambda_{\max}(G_n), \qquad \mathrm{cond}_2(G_n) = \frac{\lambda_{\max}(G_n)}{\lambda_{\min}(G_n)},$$

together with the essential infimum and supremum of the conjectured symbol, $\widetilde{G}_{\min}$ and $\widetilde{G}_{\max}$. In this way, we can observe how rapidly the minimum eigenvalue decays and, in most cases, how the maximum eigenvalues converge to the essential supremum of the spectral symbol. This provides a clear measure of the conditioning behavior as n grows (Table 3).

Case 1 - Example 2 Here $\widetilde{G}_{\max} = 2.9939$ is strictly positive. In this example, we observe a fast convergence of $\lambda_{\max}(G_n)$ and an exponential decay of $\lambda_{\min}(G_n)$, which clearly causes the condition number $\mathrm{cond}_2(G_n)$ to escalate, reaching $\mathcal{O}(10^8)$ at $n = 320$ (Table 4).

Please cite this article in press as: A. Ilyas et al., A maximal distribution result and numerical tests for geometric means of HPD GLT matrix-sequences with degenerate commuting/non-commuting GLT symbols, Linear Algebra Appl. (2025), https://doi.org/10.1016/j.laa.2025.08.004

Table 5
Extremal eigenvalues and condition numbers for **Case 2 - Example 1** (candidate symbol $\widetilde{G} \equiv 0$).

n	$\widetilde{G}_{\min}$	$\widetilde{G}_{\max}$	Min. eig.	Max. eig.	$\mathrm{cond}_2(G_n)$
40	0.00	0.00	1.2615×10^{-3}	0.511 344 01	4.0536×10^{2}
80	0.00	0.00	3.2103×10^{-4}	0.256 919 74	8.0029×10^{2}
160	0.00	0.00	8.0993×10^{-5}	0.128 771 71	1.5899×10^{3}
320	0.00	0.00	2.0342×10^{-5}	0.064 473 64	3.1695×10^{3}

Table 6
Extremal eigenvalues and condition numbers for **Case 2 - Example 2** (symbol positive on an overlap set).

n	$\widetilde{G}_{\min}$	$\widetilde{G}_{\max}$	Min. eig.	Max. eig.	$\mathrm{cond}_2(G_n)$
40	0.00	1.224 182 42	3.24×10^{-3}	1.136 583 04	3.50×10^{2}
80	0.00	1.224 182 42	1.46×10^{-3}	1.179 116 34	8.10×10^{2}
160	0.00	1.224 182 42	5.65×10^{-4}	1.201 565 62	2.13×10^{3}
320	0.00	1.224 182 42	8.19×10^{-5}	1.213 066 99	1.48×10^{4}

Case 2 - Example 1 The minimum eigenvalue appears to decay to 0 at a quadratic rate, while the largest eigenvalue converges to zero linearly, as determined by the momentary symbol. As a consequence, the growth of $\mathrm{cond}_2(G_n)$ is moderate (Table 5).

Case 2 - Example 2 Here $\widetilde{G}_{\max} \simeq 1.22$. $\lambda_{\max}(G_n)$ converges to this value and is included in the range of $\widetilde{G}$, whereas $\lambda_{\min}(G_n)$ decays linearly. This better conditioning compared to Example 2 of the first case is reasonable, since the positive perturbations we introduced to the Toeplitz matrices of this example, Equation (4.3) decay in norm more slowly than the ones in Case 1 - Example 1 (Table 6).

Zero-related statistics For each block size n we report the fraction of eigenvalues whose modulus does not exceed the fixed cutoff 0.1; see Tables 7-10. Each table lists the empirical proportion (*Prop.*≤ 0.1), the theoretical measure of the zero set of the rearranged symbol (*Target*), and the absolute difference (*Error*).

Case 1 - Example 1 The conjectured symbol is the zero function, so the target measure is 1.
The empirical value increases monotonically with n, yet within a small error. Because the number of outliers is at most $o(n)$, we expect that the proportion will converge to 1 as $n \to \infty$.

Case 1 - Example 2 Here, the zero set of the rearranged spectral symbol has measure

$$1 - \frac{1}{4\pi} \approx 0.9204.$$

Please cite this article in press as: A. Ilyas et al., A maximal distribution result and numerical tests for geometric means of HPD GLT matrix-sequences with degenerate commuting/non-commuting GLT symbols, Linear Algebra Appl. (2025), https://doi.org/10.1016/j.laa.2025.08.004

Table 7
Case 1, Example 1: proportion of eigenvalues below 0.1; target 0.

n	Prop.≤ 0.1	Target	Error
40	0.6375	1.0000	0.3625
80	0.8938	1.0000	0.1062
160	0.9438	1.0000	0.0562
320	0.9688	1.0000	0.0312

Table 8
Case 1, Example 2: proportion of eigenvalues below 0.1; target $1-\frac{1}{4\pi} \approx 0.92042$.

n	Prop.≤ 0.1	Target	Error
40	0.8750	0.9204	0.0454
80	0.8938	0.9204	0.0266
160	0.9031	0.9204	0.0173
320	0.9109	0.9204	0.0095

Table 9
Case 2, Example 1: proportion of eigenvalues below 0.1; target 0.

n	Prop.≤ 0.1	Target	Error
40	0.5000	1.0000	0.5000
80	0.5000	1.0000	0.5000
160	0.5156	1.0000	0.4844
320	1.0000	1.0000	0.0000

Table 10
Case 2, Example 2: proportion of eigenvalues below 0.1; target $\frac{17}{18} \approx 0.9444$.

n	Prop.≤ 0.1	Target	Error
40	0.7667	0.9444	0.1777
80	0.8833	0.9444	0.0611
160	0.9438	0.9444	0.0006
320	0.9448	0.9444	0.0004

The measured proportions appear to approach this value with an $\mathcal{O}(n^{-1})$ decay, the error falling below 10^{-3} by $n = 160$.

Case 2 - Example 1 Here, the expected spectral symbol is zero, but the momentary symbol perturbation, as observed in Fig. 5, produces an apparent plateau 0.5 up to $n = 320$, where the proportion jumps to 1 and the measured error vanishes. Since the momentary perturbation does not create proper outliers, as observed in Case 1 Example 2, a faster convergence can reasonably be expected in this case.

Case 2 - Example 2 In this case, the complement of the support of the rearranged distribution has measure

Please cite this article in press as: A. Ilyas et al., A maximal distribution result and numerical tests for geometric means of HPD GLT matrix-sequences with degenerate commuting/non-commuting GLT symbols, Linear Algebra Appl. (2025), https://doi.org/10.1016/j.laa.2025.08.004

$$\frac{17}{18} \approx 0.9444.$$

The empirical measure of the zero cluster converges to this value with an error that appears to follow the same power law observed in Case 2 Example 1.

5. Conclusion

We have studied the spectral distribution of the geometric mean matrix-sequence of two d-level r-block GLT matrix-sequences $\{G(A_n, B_n)\}_n$ formed by Hermitian Positive Definite (HPD) matrices, where $\{A_n\}_n, \{B_n\}_n$ have GLT symbols κ, ξ, respectively. In Theorem 3 and in Theorem 5, we have shown that the assumption that at least one of the input GLT symbols is invertible almost everywhere is not necessary when the symbols commute so that

$$\{G(A_n, B_n)\}_n \sim_{\text{GLT}} G(\kappa, \xi) \equiv (\kappa\xi)^{1/2}.$$

In this way, we have positively solved Conjecture 10.1 in [21].

On the other hand, the statement is generally false or even not well posed when the symbols are not invertible almost everywhere and do not commute, as shown in detail in several numerical experiments. This shows that Theorem 5 is maximal, so answering this time in the negative to the second item in the conclusion of [1] and to [[1], Remark 2], when both symbols are degenerate and do not commute.

Further numerical experiments are presented and critically commented in connection with extremal spectral features, linear positive operators, and in connection with the notion of Toeplitz and GLT momentary symbols. The numerical evidences open the door to further theoretical studies, which we will consider in the near future.

Finally, the study of the spectral distribution when we consider the geometric mean of more than two matrix-sequences is completely open. In this paper we have proven [[21], Conjecture 10.1]: however, when dealing with several matrix-sequences, [[21], Conjecture 10.2] is still open and for that we need normwise error estimates for using the tools in [44], while till now the convergence results in the literature have a entrywise nature (see [12] and references therein).

Declaration of competing interest

The authors declare that they have no known competing financial interests or personal relationships that could have appeared to influence the work reported in this paper.

Acknowledgements

Valerio Loi and Stefano Serra Capizzano are partly supported by “Gruppo Nazionale per il Calcolo Scientifico” (INdAM-GNCS). The work of S. Serra-Capizzano is partially

Please cite this article in press as: A. Ilyas et al., A maximal distribution result and numerical tests for geometric means of HPD GLT matrix-sequences with degenerate commuting/non-commuting GLT symbols, Linear Algebra Appl. (2025), https://doi.org/10.1016/j.laa.2025.08.004

supported by a PRIN-PNRR project (CUP J53D23003780006) and by a GNCS project (CUP E53C23001670001). Furthermore, he is grateful for the support of the Laboratory of Theory, Economics and Systems – Department of Computer Science at Athens University of Economics and Business and to the "Como Lake Center for AstroPhysics" of the University of Insubria.

Data availability

Data will be made available on request.

References

[1] D. Ahmad, M.F. Khan, S. Serra-Capizzano, Matrix-sequences of geometric means in the case of hidden (asymptotic) structures, Mathematics 13 (2025) 393, https://doi.org/10.3390/math13030393.
[2] T. Ando, C.-K. Li, R. Mathias, Geometric means, Linear Algebra Appl. 385 (2004) 305–334.
[3] N. Barakitis, V. Loi, S. Serra-Capizzano, A note on eigenvalues and singular values of variable Toeplitz matrices and matrix-sequences, with application to variable two-step BDF approximations to parabolic equations, in: Recent Dev. Spectral Approx. Theory, Springer, Cham, 2025, pp. 37–67.
[4] G. Barbarino, C. Garoni, S. Serra-Capizzano, Block generalized locally Toeplitz sequences: theory and applications in the unidimensional case, Electron. Trans. Numer. Anal. 53 (2020) 28–112.
[5] G. Barbarino, C. Garoni, S. Serra-Capizzano, Block generalized locally Toeplitz sequences: theory and applications in the multidimensional case, Electron. Trans. Numer. Anal. 53 (2020) 113–216.
[6] G. Barbarino, A systematic approach to reduced GLT, BIT Numer. Math. 62 (2022) 681–743, https://doi.org/10.1007/s10543-022-00907-8.
[7] P.G. Batchelor, M. Moakher, D. Atkinson, F. Calamante, A. Connelly, A rigorous framework for diffusion tensor calculus, Magn. Reson. Med. 53 (2005) 221–225, https://doi.org/10.1002/mrm.20334.
[8] B. Beckermann, S. Serra-Capizzano, On the asymptotic spectrum of finite element matrix sequences, SIAM J. Numer. Anal. 45 (2007) 746–769, https://doi.org/10.1137/060658809.
[9] M. Benzi, D.A. Bini, D. Kressner, H. Munthe-Kaas, C. Van Loan, Exploiting hidden structure in matrix computations: algorithms and applications, in: M. Benzi, V. Simoncini (Eds.), Lecture Notes in Mathematics, vol. 2173, Springer, Cham, 2016.
[10] R. Bhatia, Matrix Analysis, Graduate Texts in Mathematics, vol. 169, Springer, New York, 1997.
[11] R. Bhatia, Positive Definite Matrices, Princeton Series in Applied Mathematics, Princeton University Press, Princeton, NJ, 2007.
[12] D.A. Bini, B. Iannazzo, Computational aspects of the geometric mean of two matrices: a survey, Acta Sci. Math. 90 (2024) 349–389, https://doi.org/10.1007/s44146-024-00155-5.
[13] D.A. Bini, B. Iannazzo, Computing the Karcher mean of symmetric positive definite matrices, Linear Algebra Appl. 438 (2013) 1700–1710, https://doi.org/10.1016/j.laa.2011.12.042.
[14] D.A. Bini, G. Latouche, B. Meini, Numerical Methods for Structured Markov Chains, Oxford University Press, New York, 2005.
[15] J.M. Bogoya, A. Böttcher, E.A. Maximenko, From convergence in distribution to uniform convergence, Bol. Soc. Mat. Mex. 22 (2016) 695–710, https://doi.org/10.1007/s40590-016-0125-1.
[16] M. Bolten, S.-E. Ekström, I. Furci, S. Serra-Capizzano, Toeplitz momentary symbols: definition, results, and limitations in the spectral analysis of structured matrices, Linear Algebra Appl. 651 (2022) 135–168, https://doi.org/10.1016/j.laa.2022.06.017.
[17] M. Bolten, S.-E. Ekström, I. Furci, S. Serra-Capizzano, A note on the spectral analysis of matrix sequences via GLT momentary symbols: from all-at-once solution of parabolic problems to distributed fractional order matrices, Electron. Trans. Numer. Anal. 58 (2023) 136–163, https://doi.org/10.1553/etna_vol58s136.
[18] A. Böttcher, S.M. Grudsky, On the condition numbers of large semi-definite Toeplitz matrices, Linear Algebra Appl. 279 (1998) 285–301, https://doi.org/10.1016/S0024-3795(98)10092-7.
[19] M. Donatelli, C. Garoni, M. Mazza, S. Serra-Capizzano, D. Sesana, Preconditioned HSS method for large multilevel block Toeplitz linear systems via the notion of matrix-valued symbol, Numer. Linear Algebra Appl. 23 (2016) 83–119, https://doi.org/10.1002/nla.2007.

Please cite this article in press as: A. Ilyas et al., A maximal distribution result and numerical tests for geometric means of HPD GLT matrix-sequences with degenerate commuting/non-commuting GLT symbols, Linear Algebra Appl. (2025), https://doi.org/10.1016/j.laa.2025.08.004

[20] M. Fasi, B. Iannazzo, Computing the weighted geometric mean of two large-scale matrices and its inverse times a vector, SIAM J. Matrix Anal. Appl. 39 (2018) 178–203, https://doi.org/10.1137/17M1111734.
[21] C. Garoni, S. Serra-Capizzano, Generalized Locally Toeplitz Sequences: Theory and Applications. Vol. I, Springer, Cham, 2017, https://link.springer.com/book/10.1007/978-3-319-53679-8.
[22] C. Garoni, S. Serra-Capizzano, Generalized Locally Toeplitz Sequences: Theory and Applications. Vol. II, Springer, Cham, 2018, https://link.springer.com/book/10.1007/978-3-030-02233-4.
[23] B. Iannazzo, B. Jeuris, F. Pompili, The derivative of the matrix geometric mean with an application to the nonnegative decomposition of tensor grids, in: Structured Matrices in Numerical Linear Algebra, Springer, Cham, 2019, pp. 107–128.
[24] F. Kubo, T. Ando, Means of positive linear operators, Math. Ann. 246 (1980) 205–224, https://doi.org/10.1007/BF01419965.
[25] J. Lapuyade-Lahorgue, F. Barbaresco, Radar detection using Siegel distance between autoregressive processes, application to HF and X-band radar, in: Proc. 2008 IEEE Radar Conf., Rome, 2008, pp. 1–6.
[26] M. Moakher, A differential geometric approach to the geometric mean of symmetric positive-definite matrices, SIAM J. Matrix Anal. Appl. 26 (2005) 735–747, https://doi.org/10.1137/S0895479803436937.
[27] M. Moakher, On the averaging of symmetric positive-definite tensors, J. Elast. 82 (2006) 273–296, https://doi.org/10.1007/s10659-005-9008-y.
[28] N. Nakamura, Geometric means of positive operators, Kyungpook Math. J. 49 (2009) 167–181.
[29] M.K. Ng, Iterative Methods for Toeplitz Systems, Oxford University Press, New York, 2004.
[30] D. Noutsos, S. Serra-Capizzano, P. Vassalos, The conditioning of FD matrix sequences coming from semi-elliptic differential equations, Linear Algebra Appl. 428 (2008) 600–624, https://doi.org/10.1016/j.laa.2007.08.024.
[31] W. Pusz, S.L. Woronowicz, Functional calculus for sesquilinear forms and the purification map, Rep. Math. Phys. 8 (1975) 159–170, https://doi.org/10.1016/0034-4877(75)90090-5.
[32] Y. Rathi, A. Tannenbaum, O. Michailovich, Segmenting images on the tensor manifold, in: Proc. 2007 IEEE Conf. Computer Vision and Pattern Recognition, San Francisco, 2007, pp. 1–8.
[33] S. Serra-Capizzano, On the extreme spectral properties of Toeplitz matrices generated by L_1 functions with several minima/maxima, BIT Numer. Math. 36 (1996) 135–142, https://doi.org/10.1007/BF01732480.
[34] S. Serra-Capizzano, On the extreme eigenvalues of Hermitian (block) Toeplitz matrices, Linear Algebra Appl. 270 (1998) 109–129, https://doi.org/10.1016/S0024-3795(97)00318-9.
[35] S. Serra-Capizzano, Asymptotic results on the spectra of block Toeplitz preconditioned matrices, SIAM J. Matrix Anal. Appl. 20 (1999) 31–44, https://doi.org/10.1137/S0895479897322735.
[36] S. Serra-Capizzano, Spectral and computational analysis of block Toeplitz matrices having nonnegative definite matrix-valued generating functions, BIT Numer. Math. 39 (1999) 152–175, https://doi.org/10.1007/BF02510167.
[37] S. Serra-Capizzano, Some theorems on linear positive operators and functionals and their applications, Comput. Math. Appl. 39 (2000) 139–167, https://doi.org/10.1016/S0898-1221(99)00243-6.
[38] S. Serra-Capizzano, Spectral behavior of matrix sequences and discretized boundary value problems, Linear Algebra Appl. 337 (2001) 37–78, https://doi.org/10.1016/S0024-3795(01)00432-5.
[39] S. Serra-Capizzano, Distribution results on the algebra generated by Toeplitz sequences: a finite-dimensional approach, Linear Algebra Appl. 328 (2001) 121–130, https://doi.org/10.1016/S0024-3795(00)00251-7.
[40] S. Serra-Capizzano, Generalized locally Toeplitz sequences: spectral analysis and applications to discretized partial differential equations, Linear Algebra Appl. 366 (2003) 371–402, https://doi.org/10.1016/S0024-3795(02)00717-0.
[41] S. Serra-Capizzano, The GLT class as a generalized Fourier analysis and applications, Linear Algebra Appl. 419 (2006) 180–233.
[42] S. Serra-Capizzano, C. Tablino-Possio, Spectral and structural analysis of high precision finite difference matrices for elliptic operators, Linear Algebra Appl. 293 (1999) 85–131, https://doi.org/10.1016/S0024-3795(99)80009-5.
[43] S. Serra-Capizzano, P. Tilli, Extreme singular values and eigenvalues of non-Hermitian block Toeplitz matrices, J. Comput. Appl. Math. 108 (1999) 113–130, https://doi.org/10.1016/S0377-0427(99)00142-7.
[44] S. Serra-Capizzano, P. Tilli, On unitarily invariant norms of matrix-valued linear positive operators, J. Inequal. Appl. 7 (2002) 309–330, https://doi.org/10.1155/S102558340220406X.

Please cite this article in press as: A. Ilyas et al., A maximal distribution result and numerical tests for geometric means of HPD GLT matrix-sequences with degenerate commuting/non-commuting GLT symbols, Linear Algebra Appl. (2025), https://doi.org/10.1016/j.laa.2025.08.004

[45] P. Tilli, Locally Toeplitz sequences: spectral properties and applications, Linear Algebra Appl. 278 (1998) 91–120, https://doi.org/10.1016/S0024-3795(97)00319-0.
[46] P. Tilli, A note on the spectral distribution of Toeplitz matrices, Linear Multilinear Algebra 45 (1998) 147–159, https://doi.org/10.1080/03081089808818502.
[47] E.E. Tyrtyshnikov, A unifying approach to some old and new theorems on distribution and clustering, Linear Algebra Appl. 232 (1996) 1–43, https://doi.org/10.1016/0024-3795(95)00316-2.
[48] P. Vassalos, Asymptotic results on the condition number of FD matrices approximating semi-elliptic PDEs, Electron. J. Linear Algebra 34 (2018) 566–581, https://doi.org/10.13001/1081-3810.3258.
[49] L. Yang, M. Arnaudon, F. Barbaresco, Geometry of covariance matrices and computation of median, in: Bayesian Inference and Maximum Entropy Methods in Science and Engineering, in: AIP Conf. Proc., vol. 1305, Amer. Inst. Physics, Melville, 2010, pp. 479–486.
[50] F. Yger, M. Berar, F. Lotte, Riemannian approaches in brain-computer interfaces: a review, IEEE Trans. Neural Syst. Rehabil. Eng. 25 (2017) 1753–1762, https://doi.org/10.1109/TNSRE.2017.2726359.

Please cite this article in press as: A. Ilyas et al., A maximal distribution result and numerical tests for geometric means of HPD GLT matrix-sequences with degenerate commuting/non-commuting GLT symbols, Linear Algebra Appl. (2025), https://doi.org/10.1016/j.laa.2025.08.004